

1 **Insights on the spatial distribution of global, national and sub-national GHG greenhouse**
2 **gas emissions in the Emissions Database for Global Atmospheric Research (EDGAR v8.0)**

3 **Authors:** Monica Crippa², Diego Guizzardi¹, Federico Pagani², Marcello Schiavina⁶, Michele
4 Melchiorri¹, Enrico Pisoni¹, Francesco Graziosi¹, Marilena Muntean¹, Joachim Maes⁵, Lewis
5 Dijkstra^{1,5}, Martin Van Damme^{3,4}, Lieven Clarisse³, Pierre Coheur³

6
7 ¹European Commission, Joint Research Centre (JRC), Ispra, Italy

8 ²Unisystems S.A., Milan, Italy

9 ³Spectroscopy, Quantum Chemistry and Atmospheric Remote Sensing (SQUARES),
10 Université libre de Bruxelles (ULB), Brussels, Belgium

11 ⁴Royal Belgian Institute for Space Aeronomy (BIRA-IASB), Brussels, Belgium

12 ⁵European Commission, Directorate-General for Regional and Urban Policy, Brussels,
13 [Belgium](#)

14 ⁶NTT DATA, Rue de Spa, 8, 1000 Brussels, [Belgium](#)

15 Correspondence: enrico.pisoni@ec.europa.eu

16 **Abstract**

17 To mitigate the impact of greenhouse gas (GHG) and air pollutant emissions, it is of the utmost
18 importance ~~to understanding~~ where emissions ~~happen~~ occur. In the real world, atmospheric
19 pollutants are produced by ~~different various~~ human activities, ~~as from~~ point sources (e.g. power
20 plants ~~and~~ industrial facilities, ~~etc.~~); ~~but and~~ also ~~from~~ diffuse and area sources (e.g. residential
21 activities ~~and~~ agriculture, ~~etc.~~). However, as tracking all these single sources of emissions is
22 practically impossible, emission inventories are typically compiled ~~making use of~~
23 ~~country national~~ level statistics by sector, which are then downscaled at ~~the grid~~ cell level
24 using spatial information. In this work, we develop high-spatial resolution proxies ~~for use~~
25 ~~into~~ downscaling ~~the~~ national emission totals for all world countries ~~as~~ provided by the
26 Emissions Database for Global Atmospheric Research (EDGAR).

27 In particular, in this paper we present the latest EDGAR v8.0 GHG, ~~that which~~ provides readily
28 available emission data at different ~~levels of~~ spatial granularity, obtained from a consistently
29 developed GHG emissions database. This ~~is has been~~ achieved through the improvement and
30 development of high-resolution spatial proxies ~~which that~~ allow ~~thea~~ more precise allocation
31 of emissions over the globe.

32 A key novelty of this work is the ~~possibility potential~~ to analyse sub-national GHG emissions
33 ~~over the European domain territory~~; ~~but and~~ also over the ~~United States~~, China, India and other
34 high-emitting countries. These data ~~not only answer meet not only~~ the needs of atmospheric
35 modelers; but can also inform policy-makers ~~acting working~~ in the field of climate change
36 mitigation. For example, the EDGAR GHG emissions at ~~the~~ NUTS_2 level (~~nomenclature of~~
37 ~~territorial units for statistics level 2~~) over Europe contribute to the development of EU
38 ~~c~~ Cohesion policies, identifying the progress of each region towards ~~achieving~~ the carbon
39 neutrality target, as well as providing insights on the most ~~highly~~ emitting sectors. The data
40 can be accessed at <https://doi.org/10.2905/b54d8149-2864-4fb9-96b9-5fd3a020c224>,
41 specifically ~~ally~~ for EDGAR v8.0 (Crippa, 2023a) and ~~doi:10.2905/D67EEDA8-C03E-4421-~~

Formatted: English (United Kingdom)

Formatted: Font: English (United Kingdom), Ligatures: None

Formatted: Font: Ligatures: None

Formatted: Font: Ligatures: None

Formatted: Font: English (United Kingdom), Ligatures: None

Formatted: Font: Ligatures: None

Formatted: Font: (Default) Times New Roman, 12 pt, Underline, Font color: Custom Color(4,50,255), Ligatures: None

Formatted: Font: Ligatures: None

Formatted: Font: Ligatures: None

Formatted: Font: (Default) Times New Roman, 12 pt, Underline, Font color: Custom Color(4,50,255), Ligatures: None

Field Code Changed

42 [95D0-0ADC460B9658](https://doi.org/10.2905/D67EEDA8-C03E-4421-95D0-0ADC460B9658)[https://doi.org/10.2905/D67EEDA8-C03E-4421-95D0-](https://doi.org/10.2905/D67EEDA8-C03E-4421-95D0-0ADC460B9658)
43 [0ADC460B9658](https://doi.org/10.2905/D67EEDA8-C03E-4421-95D0-0ADC460B9658) for the sub-national dataset (Crippa et al., 2023b).

44

45 1. Introduction

46 Knowing where emissions are released is essential to support the design of effective mitigation
47 actions and for atmospheric modelling purposes. Emission inventories are typically developed
48 at the national level and provide sector-specific emission estimates. In order to disaggregate
49 national emissions over high-resolution grids, information on the location of the different
50 emission sources (e.g. point, linear and area sources) must be collected, and ‘spatial proxies’
51 should be developed and applied to national sector-specific emission totals to downscale them
52 over grid maps. The correct allocation of point source emissions is essential to avoid misplacing
53 high emission levels. However, gathering information on point sources covering the entire
54 globe and a wide temporal domain (1970 to present) is challenging ~~due to~~ because of limitations
55 ~~in ed~~ data availability, in the accuracy ~~in-of~~ the reporting (real location vs. legal address, etc.)
56 and in the completeness of data.

57 The Emissions Database for Global Atmospheric Research (EDGAR) provides global
58 greenhouse gas (GHG) and air pollutant emissions over the global grid_map at $0.1^\circ \times 0.1^\circ$
59 ~~degree~~-resolution, obtained through a downscaling process of national emissions using high-
60 resolution spatial data. The development and maintenance of the EDGAR grid_maps is
61 essential, since several regional and global databases rely on the EDGAR emission grid_maps
62 to disaggregate national emissions to the grid. This is the case ~~of for~~ the Community emissions
63 data system (CEDS) (Feng et al., 2020; Hoesly et al., 2018) or the European monitoring and
64 evaluation programme (EMEP) Centre on Emission Inventories and Projections (CEIP), ~~that~~
65 which supports Parties to the LRTAP Convention on Long-range Transboundary Air Pollution
66 in meeting their official gridded emission reporting requirements-obligations (CEIP, 2021).

67 This work is an update of previous EDGAR publications dealing with spatial data (Janssens-
68 Maenhout et al., 2019; Crippa et al., 2021), and describes all the new developments ~~for-in~~ the
69 spatialisation of the emissions from EDGAR_v8.0 onwards, focusing on high-emitting sectoral
70 point sources, such as power plants and industrial activities, but also on more diffuse sources
71 such as residential activities. High-resolution spatial information has been gathered at the
72 global level by combining data from the Global Energy Monitor ~~data~~, official registries and
73 satellite retrievals. The relevance of using updated spatial information is also assessed with
74 through regional case studies.

75 The purpose of this publication is to describe the EDGAR_v8.0 GHG gridded emission data
76 sets, focusing on the updates ~~of-to~~ the spatial proxies included in thiese data release. The
77 analysis of EDGAR_v8.0 emission time series (European Union, 2023; IEA-EDGAR CO₂,
78 2023) and the methodology behind emission calculations is available in Crippa et al. (2023c).

79 The main novelties of this work are (i) an update onf emission point sources using global
80 datasets (e.g. Global Energy Monitor), (ii) the development of a gap-filling method for non-

Formatted: Font: Ligatures: None

Formatted: Font: Ligatures: None

Formatted: Font: English (United Kingdom), Ligatures: None

Formatted: Font: English (United Kingdom), Ligatures: None

Formatted: Font: Ligatures: None

Formatted: Font: Subscript, Ligatures: None

Formatted: Font: English (United Kingdom), Ligatures: None

Formatted: Font: English (United Kingdom), Ligatures: None

Formatted: Font: English (United Kingdom), Ligatures: None

81 population-based sources using built-up surface information for non-residential areas-*) from
 82 the Global Human Settlements Layer (GHSL), (iii) an update of population-based proxies
 83 using the latest GHSL data, including a weighting for ~~meteorological-the temperature-~~
 84 dependent ~~need foree of heating-needs~~, and (iv) an update onf international ship tracks and
 85 weights by vessel type. In addition, information at the sub-national level (e.g. for Europe at the
 86 NUTS 2- ~~level (nomenclature of territorial units for statistics level 2)level~~) is included when
 87 developing the new spatial proxies of-for EDGAR, thus allowing a more accurate allocation
 88 and analysis of sub-national emissions. The EDGAR_v8.0 GHG global emission maps can be
 89 accessed at [doi:10.2905/D67EEDA8-C03E-4421-95D0-0ADC460B9658](https://doi.org/10.2905/D67EEDA8-C03E-4421-95D0-0ADC460B9658)
 90 <https://doi.org/10.2905/D67EEDA8-C03E-4421-95D0-0ADC460B9658> for
 91 the subnational emissions, and at ~~doi: 10.2905/b54d8149-2864-4fb9-96b9-5fd3a020c224~~
 92 <https://doi.org/10.2905/b54d8149-2864-4fb9-96b9-5fd3a020c224>
 93 for the emission grid maps at 0.1 x 0.1 degree-resolution.

94 2. Overview ofn the methodology and data sources used for updating spatial information 95 in EDGAR

96 Bottom-up global inventories (such as EDGAR) compute emissions for each sector, pollutant
 97 and year at the national level, making use of international statistics and official guidelines for
 98 emission computation (Janssens-Maenhout et al., 2019; Crippa et al., 2018). However,
 99 atmospheric modellers, policy-makers, local authorities and scientists may need to analyse
 100 spatially distributed emissions at a higher resolution than country-level data. Therefore, annual
 101 country-specific emissions are distributed over the globe making use of spatial information,
 102 representing either the exact location of point sources (e.g. power plants, industrial facilities,
 103 etc.), linear tracks (e.g. road network, ship and aeroplane tracks, etc.), and-or area sources (e.g.
 104 populated areas, industrial areas, etc.). Within the EDGAR database, over 130 proxy datasets
 105 (f) varying over time are developed to distribute the contribution of sector-specific emissions
 106 ($EM_{i,j,k}$) of each country (C) and pollutant (x) over time (t) to each grid cell ($em_{i,j,k}$) at
 107 0.1° x 0.1° resolution (about 10 km spatial resolution at the equation, considering the World
 108 Geodetic System WGS84, EPSG:4326). The Heaviside function (i.e. unit step function whose
 109 value is zero for negative arguments and 1 for positive arguments) is also used, equalling 1
 110 when the grid cell belongs to the country area, accordingly with the following formula:

$$111 \quad em_{i,j,k}(lon, lat, t, x) = EM_{i,j,k}(C, t, x) \cdot \frac{f_{i,j,k}(lon, lat, t)}{\sum_{lon, lat} (f_{i,j,k}(lon, lat, t) \cdot H_{i,j}(C, lon, lat))^2}$$

113 where

114 $H_{i,j}(C, lon, lat)$ = fraction/weight of grid cell within C ,

115 i = sector,

116 j = fuel,

(*) This information is compliant with the definition of 'building' as per the Infrastructure for Spatial Information in Europe (INSPIRE) directive: (<https://inspire.ec.europa.eu/id/document/tg/bu>) for non-residential areas (e.g. industrial or commercial facilities, warehouses, etc.) from the Global Human Settlements Layer (GHSL).

Formatted: English (United Kingdom)

Field Code Changed

Formatted: Font: (Default) Times New Roman, Font color: Custom Color(RGB(4,50,255)), Ligatures: None

Field Code Changed

Field Code Changed

Formatted: Font: Italic, Ligatures: None

Formatted: Font: Italic, Ligatures: None

Formatted: Font: Italic, Ligatures: None

Formatted: Font: Italic, Ligatures: None

Formatted: Font: Italic, Ligatures: None

Formatted: Font: Italic, Ligatures: None

Formatted: Font: Italic, Ligatures: None

Formatted: Font: Italic, Ligatures: None

Formatted: Font: Ligatures: None

Formatted: Font: Italic, Ligatures: None

Formatted: Font: Ligatures: None

Formatted: Font: Ligatures: None

Formatted: Font: Ligatures: None

Formatted: Font: Italic, Ligatures: None

Formatted: Font: Italic, Subscript, Ligatures: None

Formatted: Font: Subscript, Ligatures: None

Formatted: Font: Italic, Subscript, Ligatures: None

Formatted: Font: Italic, Ligatures: None

Formatted: Font: Italic, Ligatures: None

Formatted: Font: Italic, Ligatures: None

Formatted: Font: Italic, Ligatures: None

Formatted: Font: Italic, Ligatures: None

Formatted: Font: Italic, Ligatures: None

Formatted: Font color: Blue

117 ~~k=~~ technology.

118 Table 1 summarises the data sources and the methodology used to update spatial information
119 for each emitting sector in the EDGAR database, highlighting the most relevant and latest
120 updates compared ~~to~~ with previous EDGAR data releases. These updates apply from EDGAR
121 v8.0 onwards. Being a global database of emissions, the spatial data sources are typically
122 developed at the global level (e.g. satellite-based retrievals, ~~etc.~~); but often rely on national
123 data collection (e.g. national point-source information reported to fulfil legal requirements).
124 Therefore, the same data sources may be used by other inventory developers to update their
125 spatial disaggregation of the emission datas. In the following sections, a detailed description
126 ~~of~~ the data sources and the approach used for updating each emission sector is provided,
127 distinguishing between point sources, area sources and linear sources. For all sectors not
128 subjected to a recent revision in the EDGAR database, we refer the reader to the overview
129 Table S1 in the Supplement and the references therein.

130 A key methodological advancement in the EDGAR gridding system is the inclusion of sub-
131 national attributes for each spatial proxy and in particular for each point source. This implies
132 attaching to each point not only its exact location, expressed in longitude and latitude, but also
133 the related NUTS_2 (~~Nomenclature of territorial units for statistics~~) code (EUROSTAT, 2021)
134 for Europe or the Global Administrative layer at level_1 (GADM version_4.1). The ~~choice~~
135 ~~of~~ decision to include ~~ing~~ NUTS_2 rather than NUTS_3 information aims to enhance the
136 capability of a global database such as EDGAR to represent sub-national regional emissions in
137 support of the development of regional policies (e.g. EU cohesion reports (European
138 Commission, 2022)) or the 2040 climate impact assessment. The attribution of subnational
139 details is developed not only ~~developed~~ with an EU-oriented focus, but also for other countries
140 such as ~~the United States,~~ China, ~~and~~ India and the United States, by providing emissions at
141 the state or province level.

142 The purpose of our work is to provide readily available emission datas at the sub-national level
143 estimated in a consistent way for all countries. The EDGAR data may represent an
144 approximation for those countries with a developed statistical infrastructure (e.g. those
145 including sub-national statistics and very precise spatial proxies); however, they provide a
146 default if such data are not available, as ~~it~~ is the case for many countries in the world. In the
147 results section, case studies on sub-national emissions are presented for the EU, ~~US,~~ China,
148 ~~and~~ India and the United States.

149 3. Point sources of emissions

150 Gathering information on point sources covering the globe and spanning a wide temporal
151 domain (1970 ~~to p~~-Present) is challenging ~~due to~~ because of the limited data data-available and
152 theirity, accuracy and completeness in the reporting (real plant location vs. legal address, etc.).
153 Establishing ~~t~~he correct location of point sources is essential, since they are often super-
154 emitters (e.g. power plants for CO₂ emissions). In EDGAR_v8.0, the locations of the main
155 industrial point sources (e.g. power plants, iron and steel industries, coal mines, venting and
156 flaring activities, ~~etc.~~), which contribute ~~for~~ around half of global CO₂ emissions, haves been
157 updated using state-of-the-art information making use of from global databases, such as the
158 Global Oil and Gas Plant Tracker and Global Coal Plant Tracker of the Global Energy
159 Monitor. A complete overview of the data sources and updates included in EDGAR_v8.0 is
160 provided in Table 1.

Formatted: Font: Italic, Ligatures: None

Formatted: Font: Ligatures: None

Formatted: Font: Ligatures: None

161 However, point source databases are characterised by some limitations, ~~in terms of such as the~~
162 completeness of information on the point sources, the availability of time series ~~of for~~
163 information, the misplacement of data points compared ~~to with their real-actual~~ country
164 belonging location, etc. In EDGAR v8.0, quality ~~checks control~~ procedures are applied to
165 validate the correct location of each point source to the corresponding country or sub-national
166 attribute. Moreover, missing information is completed using assumptions on the time-lifetime
167 of power plants (i.e. 40 years) to indicatively attribute the opening or closing years for each
168 plant.

Formatted: Ligatures: None

169 No consistency checks between CO₂ emissions estimated ~~through using~~ independent methods
170 have been here performed. here However, Guevara et al. (2024) have proven that there is good
171 agreement between national CO₂ emissions from power plants as reported by EDGAR (which
172 is are based on international statistics) and plant-level inventories.

Formatted: Subscript, Ligatures: None

Formatted: Subscript, Ligatures: None

173 Atmospheric modellers require information not only ~~regarding on~~ the spatial patterns of the
174 emissions, but also on the ir temporal and vertical distribution, as described in Ahsan et al.
175 (2023), Bieser et al. (2011) and dDe Meij et al. (2006). For example, dDe Meij et al. (2006)
176 found that ~~an important role is played by~~ the vertical distribution of emissions of SO₂ and
177 nitrogen oxides (NO_x) plays an important role emissions in understanding the differences
178 between emission inventories ion calculated gas and aerosol concentrations. Accordingly, with
179 in the EMEP model, industrial point sources and power plants emissions are injected occur in
180 up to the third level (top up to 184 m), while shipping emissions happen in the first level (top
181 up to 20 m). However, addressing the vertical distribution of the emissions in beyond the
182 purpose scope of this work. In the following sections, we will describe sector by sector how
183 the most up-to-date spatial data on point sources have been collected and implemented in the
184 EDGAR database to downscale national emissions over the global grid map.

Formatted: Font: Subscript, Ligatures: None

Formatted: Font: Subscript, Ligatures: None

Formatted: Font: Ligatures: None

Formatted: Font: Ligatures: None

185

186 3.1. Power plants

187 Power plants represent a major source of fossil fuel-derived CO₂ and other GHG emissions
188 globally, nowadays contributing nowadays for around 38 % and 18 %, respectively, ~~to of~~
189 the corresponding global totals (Crippa et al., 2023c). It is therefore of utmost importance to
190 ~~correctly~~ spatially allocate these emissions correctly at the global level and understand their
191 evolution-trends over time, in order to design and implement adequate emission mitigation
192 measures.

193 In EDGAR v8.0, fuel-specific spatial proxies have been developed using data from the Global
194 Coal Plant Tracker and Global Oil and Gas Plant Tracker of the Global Energy Monitor (for
195 coal and gas) (Global Energy Monitor, 2022b, c), the Global Power Plant Database v1.3.0
196 (World Resources Institute, 2018; WRI, 2021) for oil and biofuels, the Carbon Monitoring for
197 Action database (CARMA v3.0) for autoproducers (i.e. plants and industries producing power
198 for their own use). In addition, information on autoproducers and biofuel-fired power plants in
199 Europe has been integrated using the European Pollutant Release and Transfer Register
200 (EPRTR v18) (EPRTR, 2020). For the US domain, the location of fossil fuel-fired power plants
201 is taken from the US Energy Information Administration (US EIA, 2022b), as they it represents
202 the most up-to-date source for the United States. The time frame covered by the new power
203 plant spatial proxy datasets developed in EDGAR v8.0 is 1970–2022, which includes, for each

Formatted: Font: Ligatures: None

Formatted: Font: Ligatures: None

Field Code Changed

Formatted: Font: Ligatures: None

204 plant, information on opening and closing years (~~also including~~ beyond 2022 for recently built
205 power plants), capacity, main fuel type, etc. When only partial information is available for the
206 years of operations, assumptions based on the typical lifetime of power plants ~~is-are~~ made (e.g.
207 40 years). The capacity of each power plant is used to relatively weight within a country the
208 fuel-specific emissions from power plants. An additional adjustment is performed ~~over-for~~ the
209 US ~~domain data-~~ to account for the different sulphur content in the fuel used in ~~the~~ different US
210 states based on EIA and Federal Energy Regulatory Commission utility surveys.

211 The Global Energy Monitor is chosen as the main data source for updating power plant proxies,
212 since it relies on data from public and private data sources (including the Global Energy
213 Observatory, CARMA, Platts World Energy Power Plant database, national-level trackers
214 developed by environmental organisations, as well as and various company and government
215 sources). It is validated with (i) government data on individual power plants, (ii) country
216 energy and resource plans, and government websites tracking coal plant permits and
217 applications, (iii) reports by state-owned and private power companies, (iv) news and media
218 reports, and (v) local non-governmental organisations tracking coal plants or permits. Local
219 experts are also involved in the review of coal and gas plant data. Regular bi-annual updates of
220 these databases also guarantee the possibility ~~to-of~~ include further updates in future EDGAR
221 releases. As of January 2019, the Global Coal Plant Tracker included the exact locations ~~for-of~~
222 95.3 % of operating units (6,411 out of 6,725). Independent use and validation of the Global
223 Coal Plant Tracker and Global Oil and Gas Plant Trackers is also performed by Guevara et al.
224 (2024). Figure S1 in the Supplement shows the comparison between the geographical -
225 coverage of EDGAR_v8.0 and the previous EDGAR spatial data for power plants, while
226 Figure -S2 provides a view of the global coverage of power plants in EDGAR_v8.0 by fuel
227 type.

228 Figure 1 shows the global coverage and intensity of CO₂ emissions from fossil fuel-fired power
229 plants from EDGAR_v8.0 for the years 1970 and 2022. As a general trend, the number of power
230 plants ~~strongly~~ increased strongly from 1970 to 2022 (see also Figure -2) due to ~~the~~ global
231 industrialisation ~~process-over those past~~ five decades, although the number of power plants in
232 1970 is more uncertain than that ~~of-for~~ the present day.

233 The total number of power plants grew from around 8,500 in 1970 to 13,000 in 2022, with the
234 sharpest increases occurring in China (4.5 times more) and North America (2 times more).
235 However, the intensity of the emissions has changed over the past ~~five~~ decades, depending on
236 the region. As shown in Figure 2, despite the increase in the regional number of power plants,
237 the shift towards cleaner fuels in historically industrialised regions (such as Europe and North
238 America), together with increased energy efficiency, has led to stable and lower CO₂ emissions
239 in these regions (e.g. a 13 % decrease in emissions in Europe between 1970 and 2022). ~~On~~
240 ~~the~~ In contrast, emerging regions are characterised by significantly higher emissions in 2022
241 and the use of high-carbon-content fuels, such as coal. Over the past five decades, fossil CO₂
242 emissions from power plants have increased up to 42 and 38 times in China and India,
243 respectively. Country-specific trends of-in CO₂ and GHG emissions from power plants are
244 presented in Crippa et al. (2023c).

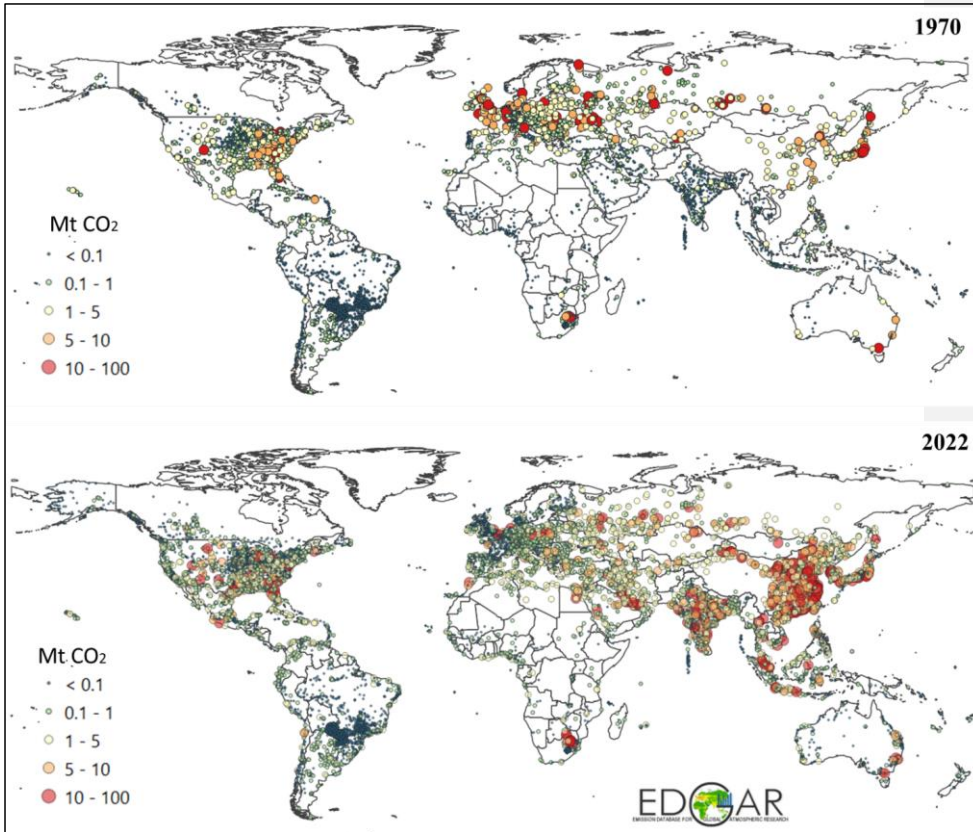
245

Formatted: Font: Ligatures: None

Formatted: Not Highlight

Formatted: Not Highlight

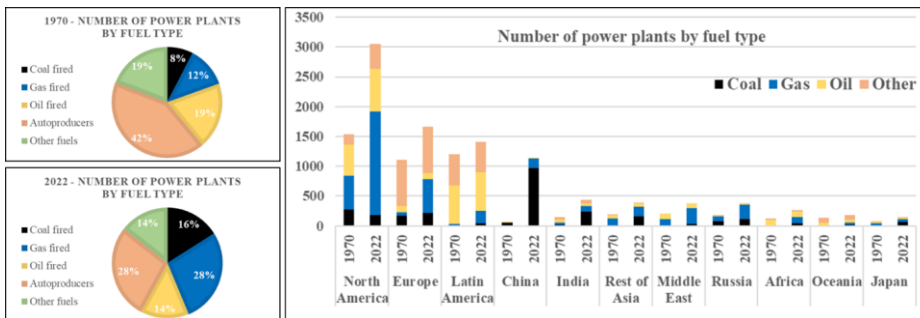
Formatted: Font: Ligatures: None



246

247

248 **Figure 1 – CO₂ emissions from fossil fuel-fired power plants in 1970 and 2022 from EDGAR_v8.0. The size of the circles is proportional to the magnitude of the emissions.**



249

250

251 **Figure 2 – Evolution of Increase in the total number of power plants (including fossil fuel- and bio-fuel-fired plants) from 1970 to 2022 by world region, as included in the updated EDGAR spatial proxies.**

252

253

254 **3.2. Industrial facilities and other point sources**

255 Industrial activities cover a wide range of sectors encompassing the production of iron and
256 steel, cement, glass, metals, chemicals ~~and~~, fertilisers ~~and the~~, use of solvents, but also intensive
257 animal farming (see [Section 3.4](#)). Gathering information on industrial activities (e.g.
258 production, capacity, location of the facilities, ~~etc.~~) at the global level is challenging, ~~also due~~
259 ~~to~~ ~~in part because of~~ confidentiality and data protection issues. For this reason, we focused not
260 only on the ~~update~~ ~~ing~~ of information on industrial point sources (when available); but also on
261 ~~the~~ ~~improvement of~~ the gap-filling method for all industrial activities ~~in case of~~ ~~if data are~~
262 incomplete or missing ~~data~~ (as discussed in detail in [Section 3.5](#)). In EDGAR_v8.0, we
263 included the latest ~~European Pollutant Release and Transfer Register~~ [EPRTTR](#) (EPRTTR_v18)
264 locations for all industrial facilities (with the exception of power plants, iron and steel facilities,
265 and coal mines, for which dedicated spatial proxies have been developed at the global level).
266 Several manual adjustments were ~~implemented~~ ~~made~~ to overcome data quality issues related
267 ~~with~~ ~~to~~ missing spatial information and inconsistencies. The analysis of the EPRTTR dataset
268 also inspired the idea of attributing only a fraction of the emissions to the reported point
269 sources. This is ~~also~~ justified by the fact that industrial facilities have to report their emissions
270 only if they fall above a certain threshold. The fraction of the emissions to be allocated to the
271 available point sources is determined through the ratio between ~~the~~ EPRTTR emissions
272 (typically of CO₂) and the corresponding EDGAR emissions. When the ratio is 1, all emissions
273 are allocated to the point sources; when the ratio is lower than 1, the complementary fraction
274 is then attributed to the gap-filling grid (i.e. non-residential proxy as defined in [Section 3.5](#)).

275 In EDGAR_v8.0, we have also updated the global locations of iron and steel plants, which are
276 among the most energy-intensive industries. The Global ~~S~~ ~~steel~~ ~~P~~ ~~plant~~ ~~T~~ ~~racker~~ of the Global
277 Energy Monitor (2022d) was used as a data source ~~due to~~ ~~because of~~ its global and temporal
278 completeness (1970 ~~to~~ present). The installed capacity was used to weight the relative
279 contribution of each iron and steel plant, although it may represent an approximation ~~for~~ ~~of~~ the
280 real capacity in use. A map of iron and steel production plants in 1970 and 2022 is presented
281 in [Figure 3](#). The number of iron and steel plants increased around ~~10~~ ~~ten~~ fold over the last five
282 decades (from 77 to 728) with the sharpest increases in China (~~5~~ ~~five~~ fold) ~~and~~, ~~USA~~ ~~the~~ ~~United~~
283 [States](#) and India (2.7-fold).

284 Coal ~~m~~ ~~M~~ ~~ines~~ are also a relevant source of fugitive emissions of GHGs and air pollutants (e.g.
285 volatile organic compounds). In EDGAR_v8.0, we updated the information on coal mines at
286 the global level using the Global Coal Mine Tracker of the Global Energy Monitor (2022a)
287 complemented with the ~~Energy Information Administration~~ [EIA](#) data for the [United States](#) (US
288 EIA, 2022a). For countries not covered by these data sources, we relied on the previous
289 EDGAR spatial proxies including data from the [United States](#) Geological Survey (USGS,
290 2019). More specifically, we included information on surface and underground mines: ~~for~~ both
291 ~~for~~ hard and brown coal.

Formatted: Font: Subscript, Ligatures: None

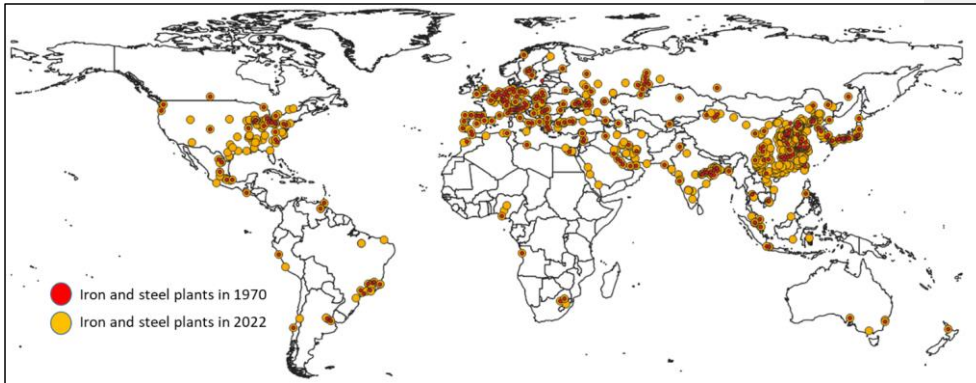


Figure 3 – Global locations of iron and steel plants in 1970 and 2022.

3.3. Venting and flaring

Gas flaring is the burning of the natural gas that results from oil extraction. Although this practice is highly polluting and represents a waste of resources, it ~~is~~ still ~~is~~ takes place in several countries ~~due to~~ because of economic constraints and ~~the a~~ lack of appropriate legislation ~~in several countries~~. Flaring takes place ~~at~~ both ~~as~~ on-shore and off-shore ~~activities~~ installation, and it is a source of GHG and air pollutant emissions.

Global CO₂ emissions related ~~with to~~ flaring accounted for 276 Mt in 2022, of which 76 % ~~was~~ emitted by 10 countries, namely Russia (18 % of the global total), Iraq (13 %), Iran (12 %) and Venezuela (7 %), followed by Algeria, ~~United States A~~, Mexico, Libya, Nigeria and China. Although this emission source represents only 0.8 % of global CO₂ emissions, it is particularly relevant for certain regions ~~in of~~ the world, such as Venezuela (20 % of the ~~CO₂ country's~~ total CO₂ emissions), Iraq (18 %), Libya (17 %), Algeria (10 %) and Nigeria (9 %). Considering the relevance of venting emissions and the potential ~~of for~~ control measures, it is essential to ~~best~~ accurately quantify and attribute ~~the correct georeference for~~ this source ~~to the correct location~~. Flaring emissions can also be localised and quantified ~~through using~~ space-borne measurements (Elvidge et al., 2017; NOAA, 2017). In EDGAR_v8.0, data from the World Bank *Global Gas Flaring Tracker Report* (2023) were used ~~both~~ for estimating ~~both~~ the emissions and ~~the~~ location of global flaring activities from 2012 to 2022. These spatial data were also used as a best approximation to spatially distribute emissions from venting, which is the controlled release of natural gas without ~~it~~ being burned, although the two activities may not overlap. The resulting ~~map of~~ CO₂ emissions ~~map~~ in 2012 and 2022 is ~~reported~~ shown in Figure -4.

Formatted: Font: Subscript, Ligatures: None

Formatted: Font: Subscript, Ligatures: None

Formatted: Font: Ligatures: None

Formatted: Font: Italic, Ligatures: None

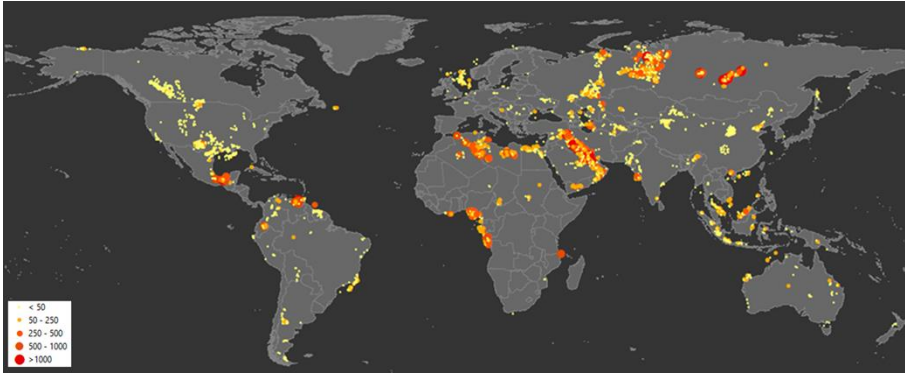


Figure 4 – Global map of CO₂ emissions (kt) from flaring in 2022.

3.4. Intensive livestock and fertiliser-manufacturing industries

Agriculture includes a variety of activities that are typically distributed over large areas (e.g. crop areas, animal pastures, etc.). However, several agricultural activities can be defined as hot-spots or point sources and include intensive animal farming and manure management practices. In a broader sense, we also allocate to this sector the also-fertiliser-manufacturing production-industry, which represents an important source of NH₃ and N₂O. In EDGAR v8.0, the infrared atmospheric sounding interferometer (IASI) satellite-derived NH₃ point source database (Van Damme et al., 2018; Clarisse et al., 2019) is included to map emissions from animal farming and fertiliser production emissions with yearly information for the period 2008–2022. It includes 270 agricultural hot-spots and 251 synthetic NH₃ production facilities of synthetic NH₃ worldwide. Since the NH₃ point source database includes only hot-spots, we decided to allocate to these points only a fraction of the total emissions for that sector and country derived from approximate estimates of NH₃ emission fluxes from IASI measurements, while distributing the remaining fraction to livestock density maps formerly available in EDGAR. Similarly to what was done for other industries, for Europe, intensive livestock and fertiliser production point sources and fertiliser production industries were taken from EPRTR v18. Similarly, the satellite-based information on fertiliser industries was integrated into the previous EDGAR proxy for this sector. This update represents a significant improvement in representing nitrogen-related hot-spots (Van Damme et al., 2018) compared to with former earlier EDGAR releases which mostly used animal density as a proxy (see Table S1), albeit considering taking into account that the uncertainty of IASI information is around 50 %. A snapshot of N₂O emissions from manure management at the global level and in Europe, where intensive livestock activities appear as emission hot-spots, is shown in Figure 5.

Formatted: Font: Subscript, Ligatures: None

Formatted: Font: Subscript, Ligatures: None

Formatted: Font: Subscript, Ligatures: None

Formatted: Font: Subscript, Ligatures: None

Formatted: Font: Subscript, Ligatures: None

Formatted: Font: Subscript, Ligatures: None

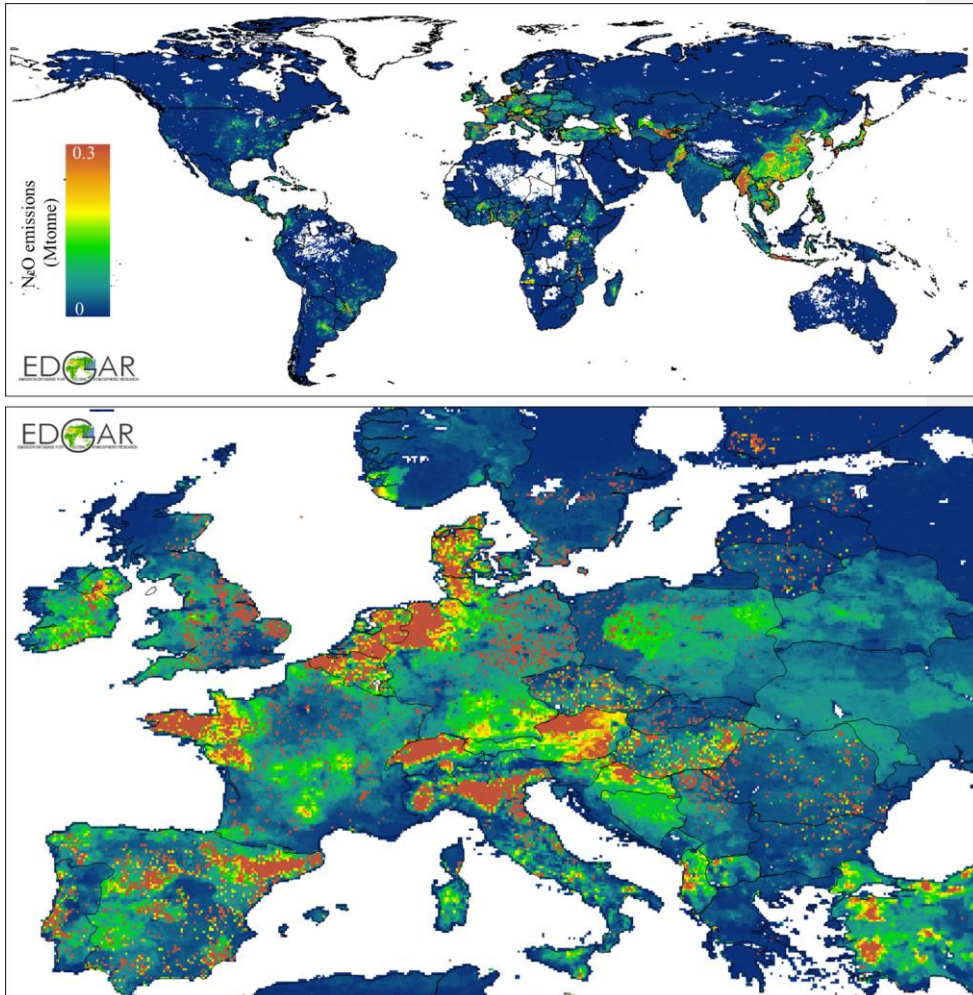
Formatted: Font: Subscript, Ligatures: None

Formatted: Font: Ligatures: None

Formatted: Font: Ligatures: None

Formatted: Font: Ligatures: None

Formatted: Font: Subscript, Ligatures: None



341
 342 **Figure 5 – N₂O emissions from manure management at [the global level](#) and in Europe, where intensive**
 343 **livestock activities appear as emission hot-spots.**

344 **3.5. Gap-filling missing information ~~of~~for point sources**

345 A significant improvement is represented by the development and use of a new spatial proxy
 346 to gap-fill missing information for all industry-related emissions. Until EDGAR_v7.0,
 347 population-related proxies were used as backup information when no spatial data were
 348 available to represent the emissions for a sector within a country (Crippa et al., 2021). However,
 349 here we decided to use the non-residential built-up surface information developed by the [Global](#)
 350 [Human Settlements Layer \(GHSL\)](#) (Pesaresi and Politis, 2023; European Commission, 2023)
 351 as a backup proxy to distribute the emissions of all the activities not related to small-scale
 352 combustion for which no point source information was available (even for individual
 353 countries). This methodological assumption is a key novelty of this work ~~due to~~because of its

Field Code Changed

Formatted: Font: Ligatures: None

354 application at the global level. However, it is in line with methodologies already applied in
355 regional inventories, such as in Europe (Kuenen et al., 2022), where the ~~Corine~~ORINE L and
356 ~~Cover-use~~ dataset is used to spatially allocate emissions to areas with industrial activity, thus
357 supporting the validity of this assumption.

358 For certain sectors and regions, this non-residential gap-filling proxy is also used to allocate a
359 fraction of the emissions of certain sectors (~~refersee~~, for example, ~~to~~ the industrial facilities
360 section for Europe). The overall effect of using this new proxy is a change in the industrial
361 contribution over densely populated areas, which was previously higher in EDGAR ~~compared~~
362 ~~to~~ ~~than in~~ other inventories ~~in particular~~ over Europe ~~in particular~~ (Thunis et al., 2023). Figure 6
363 shows CO₂ emission maps from manufacturing industries obtained ~~in from~~ EDGAR_v7.0 and
364 ~~EDGAR~~v8.0. This ~~comparison~~ figure highlights the implications of using different gap-filling
365 proxies for the industrial sector, and in particular contrasts those based on population (EDGAR
366 v7.0) with the new ones based on non-residential built-up surface data (~~used in~~ EDGAR_v8.0).

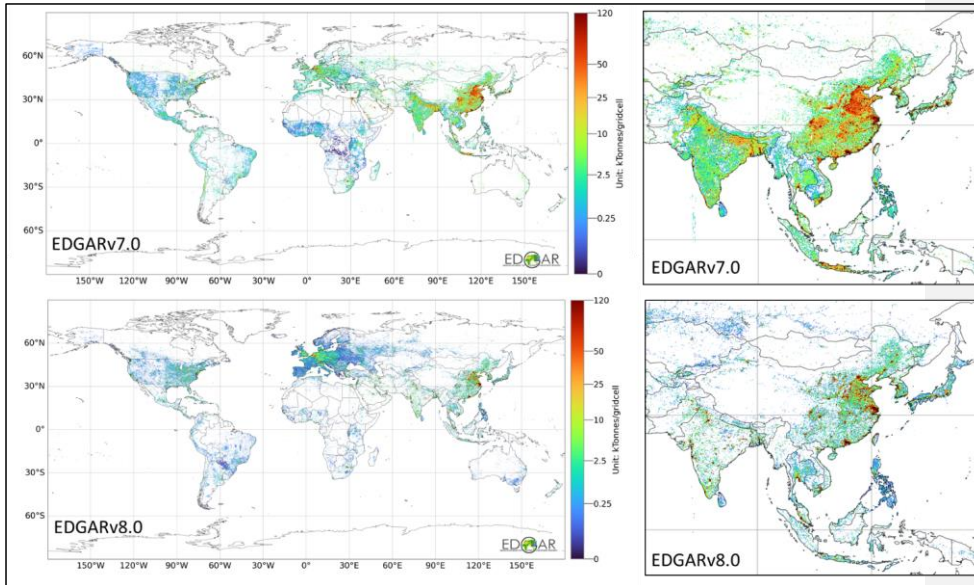
367 Overall, using non-residential built-up information to allocate emissions of industrial activities
368 to complement point source information leads to lower emission levels ~~being~~ allocated to urban
369 areas and a less densely distributed map over certain regions (e.g. China, India, ~~etc.~~). Figure S3
370 shows the impact of this update on global fossil ~~fuel-derived~~ CO₂ emissions from the industrial
371 sector over global ~~f~~Functional ~~u~~Urban ~~a~~Areas (FUAs) in 2022. The share of CO₂ industrial
372 emissions ~~to of~~ the national total over FUAs is typically higher, on average by around 30 %, in
373 EDGAR_v8.0 than in EDGAR_v7.0 for several developing countries (e.g. Africa, ~~India~~, South
374 America, ~~India~~, ~~etc.~~) ~~due to because of~~ the presence of industrial point sources and non-
375 residential activities still close to urban areas. ~~On the other hand~~ ~~However~~, lower emissions
376 from industries (on average around 20 % less) are found in many industrialised regions (e.g.
377 Europe, ~~USA~~, Oceania, ~~United States~~) ~~due to because of~~ the displacement of industrial activities
378 in remote areas or outside the FUAs. This result represents the effect of using non-population-
379 based proxies for industrial emissions in EDGAR_v8.0 compared ~~to with~~ previous EDGAR
380 proxies.

Formatted: Font: Ligatures: None

Field Code Changed

Formatted: Font: Subscript, Ligatures: None

Formatted: Font: Subscript, Ligatures: None



382 Figure 6 – CO₂ emissions from industrial combustion in 2021 from EDGAR v7.0 (top) and v8.0 (bottom),
 383 showing the impact of the gap-filling proxies used for industrial sources.

Formatted: Font: Subscript, Ligatures: None

384 4. Linear sources of emissions: international shipping

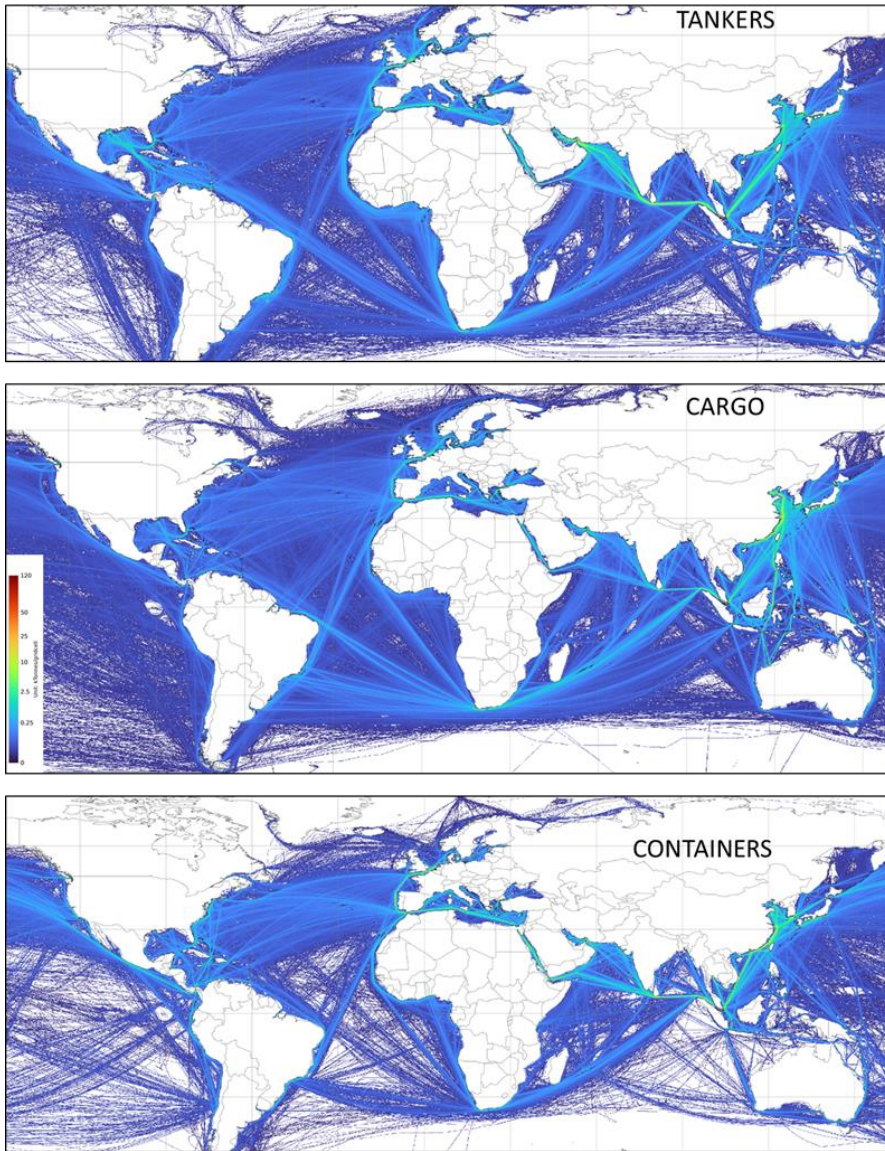
385 Since EDGAR_v6.0, international shipping emissions ~~are-have been~~ distributed using the [Ship](#)
 386 [Traffic Emission Assessment Model \(STEAM_3\)](#) (~~Ship Traffic Emission Assessment Model~~
 387 ~~model~~ from the Finnish Meteorological Institute (Jalkanen et al., 2012; Johansson et al., 2017)
 388 and this approach has remained unchanged in EDGAR_v8.0. Emissions are distributed on a
 389 yearly basis from 2000 to 2018, including multi_vessels information (cargo, container, fishing,
 390 passenger cruisers, service, tankers, vehicle carriers, miscellaneous). Compared ~~to-with~~
 391 the previous EDGAR proxy, the use of the STEAM data allows a better representation of the
 392 ~~evolution-intrend over~~ time ~~of-in the~~ international shipping emissions, differentiating on an
 393 annual basis the variation ~~of-in~~ the routes and their intensity for the different vessels
 394 consistently with the information available in EDGAR (see [Figure-7](#)). Only data covering sea
 395 areas are included, since inland data over big rivers or lakes is not robust enough to be included
 396 in EDGAR. Information on ~~eEmission cControl aAreas (ECAs)~~, and in particular on sulphur
 397 emission control areas (~~SECAs~~) and NO_x emission control areas (~~NECAs~~), ~~are-is~~ not yet
 398 included, although this may be considered ~~for-in~~ future updates of EDGAR. A comparison
 399 ~~between-of the~~ international shipping intensities ~~that-are~~ available in EDGAR before and after
 400 this update is presented in [Figure-S4](#) of the Supplement.

401 Figure 8 focuses on three main vessel types, representing the largest fraction of GHG emissions
 402 from international shipping in 2022 and contributing specifically ~~for~~ around 22 % (tankers),
 403 24 % (containers) and 28 % (cargo) ~~to-of~~ total international shipping GHG emissions. The
 404 impact of using the STEAM data to develop the new spatial proxies for international shipping
 405 is shown in [Figure-8](#), ~~where-which presents the-a~~ comparison between EDGAR_v5.0 and
 406 EDGAR_v8.0 CO₂ emissions from the three main vessel types over the different ~~o~~Oceans and

Formatted: Font: (Default) Times New Roman, Subscript, Ligatures: None

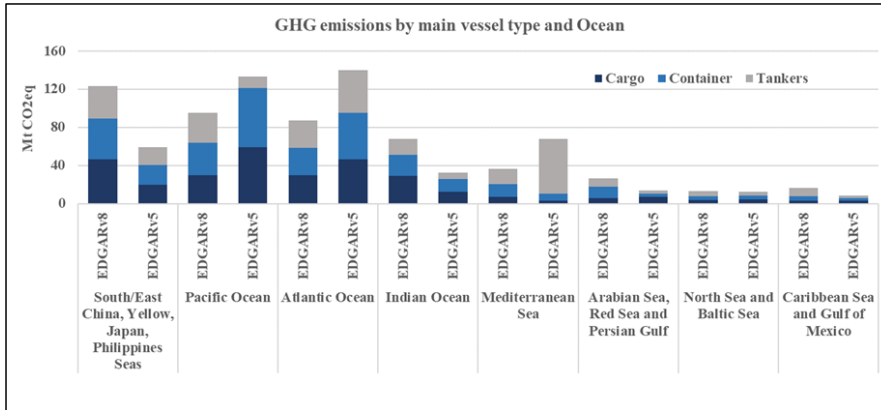
407 ~~s~~Seas ~~is presented~~. EDGAR_v5.0 used an in-house EDGAR proxy based on Wang et al. (2008),
408 improved with ~~LRIT~~ (~~L~~ong-~~R~~ange ~~I~~dentification and ~~T~~racking) information (Alessandrini
409 et al., 2017) for European seas, as described in Janssens-Maenhout et al. (2019). EDGAR_v5.0
410 proxies were allocating most of the international shipping emissions over the Atlantic and
411 Pacific Oceans, while the new proxies of EDGAR_v8.0 allocate the largest portion of these
412 emissions (40 %) over the ~~s~~Seas around China, Japan and ~~the~~ Philippines. The relative share
413 of tanker emissions over the Mediterranean Sea is also very different between the two versions,
414 with the largest contribution (85 %) ~~among from~~ the three ~~categories~~ considered ~~categories~~ in
415 EDGAR_v5.0. Emissions allocated to the Gulf of Mexico and Arabian Sea are two times higher
416 ~~when~~ using the STEAM_~~b~~-based proxies in EDGAR_v8.0.
417

418



419
 420
 421
 422

Figure 7 – International shipping GHG emissions in (2021) with showing the ship tracks for tankers, cargo vessels and containers and cargo vessels as in EDGAR v8.0.



423
 424 **Figure 8 – Comparison of GHG emissions from international shipping in (2022) by main vessel type and**
 425 **ocean or sea from EDGAR v5.0 and EDGARv8.0. Fishing, service-s and passenger-related emissions**
 426 **are excluded from this comparison.**

427 **5. Area sources of emissions**

428 **5.1. Residential activities**

429 Small-scale combustion emissions are mostly related ~~with-to~~ non-industrial activities, such as
 430 those from the residential, commercial, ~~and~~ agricultural ~~and~~ fishing sectors. Therefore,
 431 population-based spatial proxies are often used to downscale national emissions. EDGAR_v8.0
 432 aims to couple population distribution with heating degree-days, since the amount of emissions
 433 is not only dependent on the number of people living ~~over-in a certain area-s~~, but also on the
 434 meteorological conditions and the ~~need for~~ heating ~~needs for~~ indoor spaces. Residential
 435 emissions are therefore distributed considering both population intensities and heating needs,
 436 with varying profiles from 1970 to 2022. EDGAR_v8.0 includes the latest population grid maps
 437 developed by ~~the~~ Global Human Settlements, GHS-POP R2023A (Schiavina et al., 2023b;
 438 Freire et al., 2016), which comprise residential population information for 12 epochs, over
 439 1975–2020 with ~~five~~5-year time steps and projections to 2025 and 2030 obtained by
 440 distributing census data from CIESIN GPWv4.11 over global grid_maps. GHS-POP R2023A
 441 data at 30 arc-seconds (WGS84, EPSG:4326) (or about 1 km) spatial resolution were used to
 442 develop the corresponding spatial proxies in EDGAR. Population density is then calculated for
 443 each grid_cell and ~~it-is~~ used as a proxy to allocate household emissions over populated areas.
 444 Small-scale combustion activities related ~~with-to~~ agriculture are distributed using rural
 445 population maps obtained from the GHS-SMOD R2023 product (including only low_ and very
 446 low-density rural grid cells) (Schiavina et al., 2023a). For missing years, the closest population
 447 map to each epoch is taken (e.g. for the years 2001 and 2002 the population map from 2000 is
 448 used, while for the years 2003 and 2004 the 2005 map is used).

449 To account for the effect of the weather (ambient temperature) on heating needs in the
 450 residential sector, heating degree-days (HDDs) ~~have-been~~were computed using the 2_meters
 451 ~~surface air~~ temperature data with hourly time resolution and 1_degree spatial resolution using
 452 the Copernicus ERA5 atmospheric reanalysis produced by ~~the~~ European Centre for Medium-
 453 ~~Range~~ Weather Forecasts for the years 1970–2022

Formatted: Font: Ligatures: None

454 (<https://cds.climate.copernicus.eu/cdsapp#!/dataset/reanalysis-era5-single-levels?tab=form>).
455 HDD_s is the cumulative number of degrees by which the mean daily temperature falls below a
456 reference temperature (usually 18_°C or 19_°C, which is adequate for human comfort). HDD_s
457 were calculated following the methodology described by Spinoni et al. (2018) and assuming a
458 reference temperature of 18_°C. Cooling ~~d~~Degree-d-Days-(CDD) are not included in the
459 development of the spatial proxies, since they are mainly related ~~with-to~~ electricity
460 consumption rather than to fuel combustion in the residential sector. An additional weight ~~is~~
461 ~~therefore added~~ to the population distribution ~~is therefore added by using~~ the HDD metric, thus
462 increasing the emissions arising in colder regions ~~subjected to more~~with a greater need for
463 heating ~~needs rather~~ than in warm areas for the same amount of population.

464 Our approach does not aim to identify and represent ~~the~~ heating habits for all countries, ~~while~~
465 ~~but modulating~~ within a single country ~~modulates~~ the ~~differences in~~ combustion of fuels for
466 ~~for example, e.g.~~ heating purposes due to the different ~~mean~~ temperatures across latitudes
467 (climatic zones). Country ~~populations~~ies may ~~in fact also~~ have different habits in ~~terms of~~
468 turning on and off their heating systems, thus requiring the use of different reference
469 temperature values in the calculation of HDD_s (Atalla et al., 2018), ~~which is not taken into~~
470 account here. The process ~~to of~~ building the residential proxy in EDGAR is shown in Figure-
471 9.

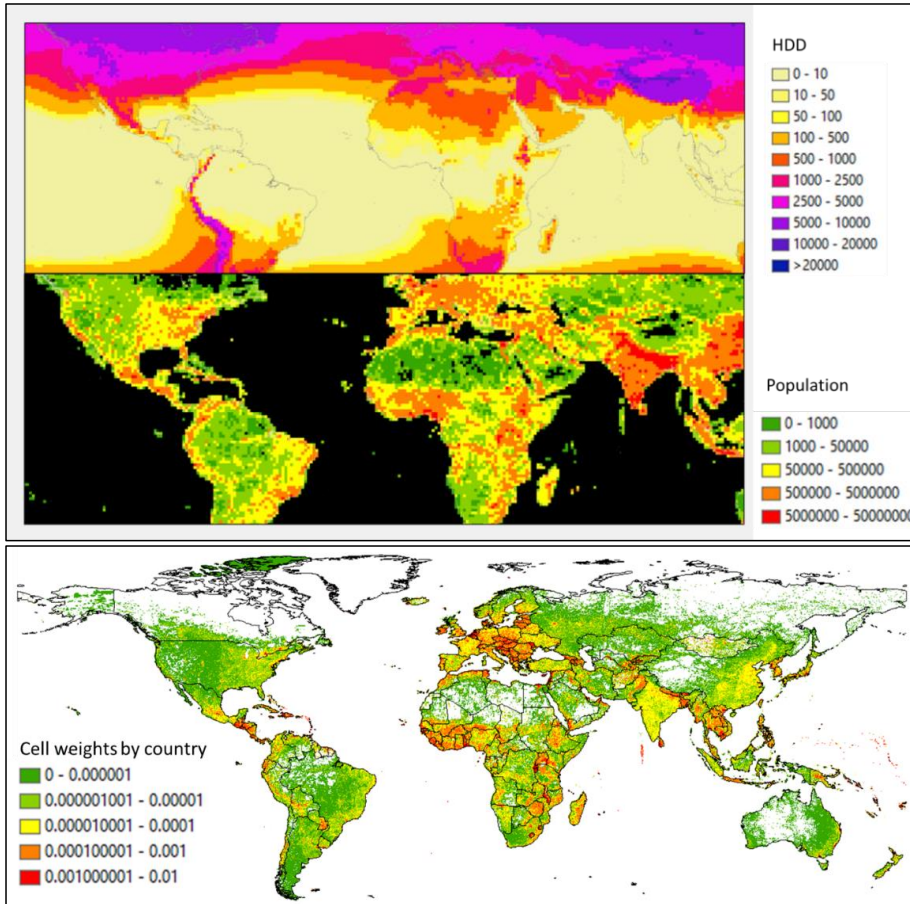
Formatted: Font Ligatures: None

Formatted: Not Highlight

Formatted: Font Ligatures: None

Formatted: Font Ligatures: None

Formatted: Font Ligatures: None



472

473

474 Figure 9 – Coupling [heating degree days](#) ([HDDs](#)) ([atop](#)) and population density ([bmiddle](#)) as a proxy
 475 ([ebottom](#)) to downscale residential emissions. Data [refer to are for](#) the year 2020.

476

477 **6. Results**

478 The purpose of this work [was](#) to describe the methodological improvements included in
 479 EDGAR_v8.0 linked to the update of the spatial data used to downscale country_ and sector_
 480 specific emissions. In addition, a specific focus is dedicated to case studies showing the
 481 relevance of understanding the [evolution of trends in](#) GHG emissions at [the](#) sub-national level
 482 in order to support the development of regional climate mitigation and adaptation policies
 483 (Kuramochi et al., 2020). [Therefore,](#) ~~t~~the reader can refer to Crippa et al. (2023c) for [the a](#)
 484 description of country_ and sector-specific GHG emission trends at [the](#) global level. In the
 485 following sections, insights on the global distribution of GHG emissions [as well as and](#)
 486 their sub-national features are described.

487 **6.1. Global [GHG](#) [greenhouse gas](#) emissions in EDGAR_v8.0**

488 Figure 10 shows global GHG emissions in 2022 as a result of the EDGAR_v8.0 gridding
489 process, while Figure 11 reports the same emissions at the country and sub-national level.
490 Complementary figures are also reported-presented in the Supplement. The maps in
491 (Figures_S5-S8) showing the evolution of trends in global emissions of GHGs and fossil fuel-
492 derived CO₂, CH₄ and N₂O global emission maps from 1970 to 2022.

Formatted: Font: Ligatures: None

Formatted: Not Highlight

Formatted: Font: Ligatures: None

493 The main strength and novelty of EDGAR_v8.0 is related with-to the production of a global
494 GHG emission database at different levels of granularity in-to support of local, regional and
495 global climate actions. The high-spatial-resolution global maps are available at 0.1° × 0.1°
496 resolution WGS84 (EPSG:4326), about 10 km spatial resolution at the equator, as both as-emissions
497 and emission fluxes (.txt and .NetCDF files, https://edgar.jrc.ec.europa.eu/dataset_ghg80)
498 fulfilling the requirements of the global atmospheric modelling community but also bridging
499 bottom-up and top-down (mostly satellite-based) GHG emission estimates (see Figure-10).

500 EDGAR_v8.0 allows full flexibility in the aggregation of emissions at the sub-national level,
501 thus supporting the analysis of the spatio-temporal variability of the emissions not only at the
502 grid-cell level but also over wider administrative domains, or areas of interest such as urban
503 centres (Melchiorri, 2022). A second key product from EDGAR_v8.0 is represented by GHG
504 emissions at the sub-national level using the Global Administrative layer version_4.1
505 (https://gadm.org/download_country.html) at level_1 and the NUTS_2 level for the EU
506 extended geographical domain, as shown in Figure-11.

507 Looking at province_ or city-scale emissions requires not only associating, e.g. for example,
508 point sources to the NUTS_3 level but also relying on an approach different approach from the
509 downscaling of national totals, which may include the use of statistical information available
510 over smaller territorial units. Therefore, considering the current purposes of EDGAR, the
511 NUTS_2 level represents the right balance between the accuracy of the final emission data and
512 downscaling of national totals. The relevance of including not only country-specific details,
513 but also sub-regional information is essential when doing emission data extraction at the sub-
514 national level, thus avoiding border issues. Some inventory compilers (Kuenen et al., 2022),
515 report point source information as just as-points without distributing them over a grid map with
516 a certain resolution. This approach is accurate, since it provides the exact geographical
517 coordinates of individual facilities; however, it does not reduce data extraction issues, since the
518 allocation of a specific point to a certain grid cell may fall between-at the borders of, for
519 example, e.g. two or more regions.

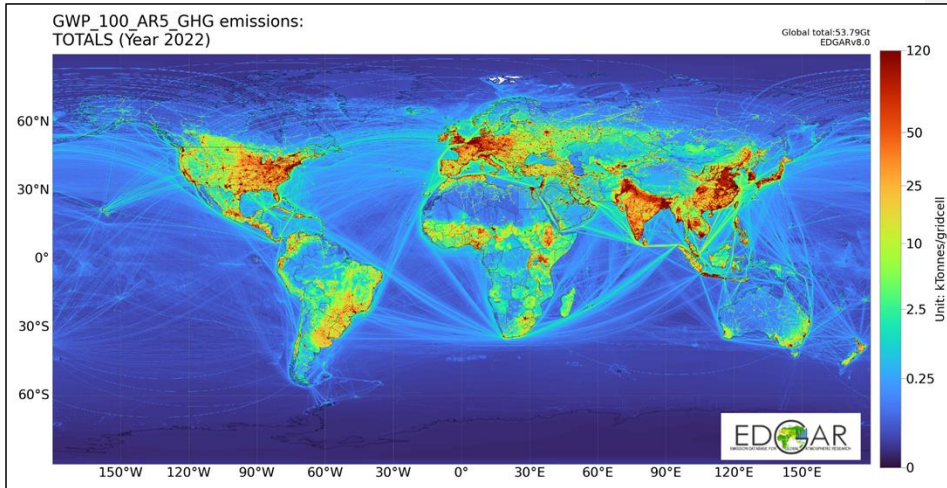
Formatted: Font: Ligatures: None

Formatted: Font: Ligatures: None

520 Another challenge that we address with this new gridding approach is related with-to the
521 harmonisation of national and sub-national data. Local and regional inventories are often
522 developed independently, therebefore, undermining the possibility to-of eollate combining
523 together sub-national emission data to retrieve the national values. The challenge of using
524 different and not coherent/unharmonised databases is overcometaken by the EDGAR database,
525 being-as users are able to work consistently work both at both the national and regional levels,
526 thus offering the m user the possibility to-of working across different geographical scales. This
527 is achieved through the downscaling of national emission data to sub-national data, making
528 use of high-spatial-resolution proxies, as discussed in this paper. In the next sSections 6.2 and
529 6.3, case studies over-in the European, American and Asian domains are discussed more in
530 detail.

Formatted: Font: Ligatures: None

531

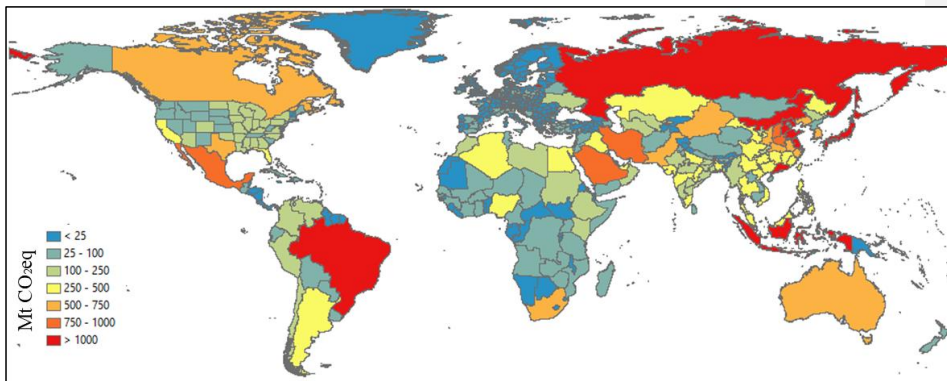


532

533

Figure 10 – Global GHG (expressed in kt CO₂e equivalent) emission map in 2022 from EDGAR v8.0.

Formatted: Font: Subscript, Ligatures: None



534

535

536

Figure 11 – Global GHG emissions by at the country-national and sub-national levels in 2022 based on EDGAR v8.0.

537

538

6.2. Sub-national emissions: the EU case

539

540

541

542

543

544

545

546

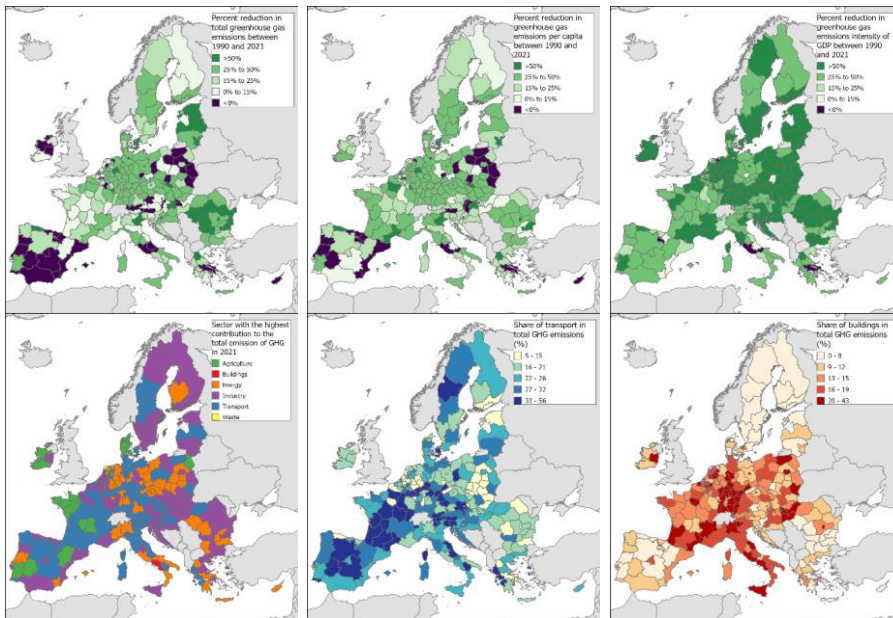
547

Climate and environmental territorial policies require robust and consistent knowledge of greenhouse gas (GHG) and air pollutant emissions at the sub-national level (e.g. NUTS_2). No sub-national official reporting is available and the high-spatial-resolution data of available from EDGAR fill this knowledge gap. EDGAR sub-national GHG emissions are used as a reference by the European Commission in Cohesion Reports (European Commission, 2022), the European semester process or and Climate Action territorial analysis. Figure 12 shows how GHG emissions at the NUTS_2 level have changed from between 1990 to and 2021 both in absolute, per capita and per GDP-gross domestic product terms. Out of 242 EU regions, 155 regions have shown a downwards trend in emissions since 1990, while it is found for and 206

548 and 204 regions [have done so](#) since 2005 (on average -1.27% per year) and 2010 (on
 549 average -1.35% per year), respectively. However, in 2021, only 34 regions [reached-achieved](#)
 550 [GHG emissions of less than 5 t-CO₂equivalent/person](#), which [corresponds to](#) the average
 551 value needed to achieve the 2030 EU climate targets. The [sectors most-contributing most](#)
 552 [sectors](#) to total EU GHG emissions in 2021 are power generation (27%), industry (23%),
 553 transportation (20%), buildings (14%) and agriculture (11%), showing that the different
 554 regions in the EU have different transition challenges. For example, when looking at the
 555 NUTS_2 level (see [Figure-12](#), [bottom middle bottom-panel](#)) the transport sector [is](#) often
 556 [represents](#) the sector with the largest contribution at [the](#) regional level, in particular in rural
 557 regions of Spain, France, Italy, ~~or~~ and Germany. Figure 12 (bottom right panel) also shows the
 558 share of GHG emissions arising from small-scale combustion (buildings sector) at the NUTS_2
 559 level, highlighting several regions for which this sector contributes more than 15–20% to the
 560 regional total.

Formatted: Font: Subscript, Ligatures: None

561



562

563 **Figure 12 – Relative change of in EU European GHG emissions by NUTS_2 level between 1990 and 2021 (top**
 564 **panels). Sectoral contribution of to EU European GHG emissions by NUTS_2 level in 2021 (bottom panels).**
 565 **The sector with the highest contribution in 2021 for each NUTS_2 region is shown in the map on the left**
 566 **panel. The share-contribution of GHG emissions from transport (middle panel) and buildings (right panel)**
 567 **to total emissions in 2021 in the EU Europe by NUTS_2 level is also shown.**

568

569 6.3. Sub-national emissions in the United States, China and India

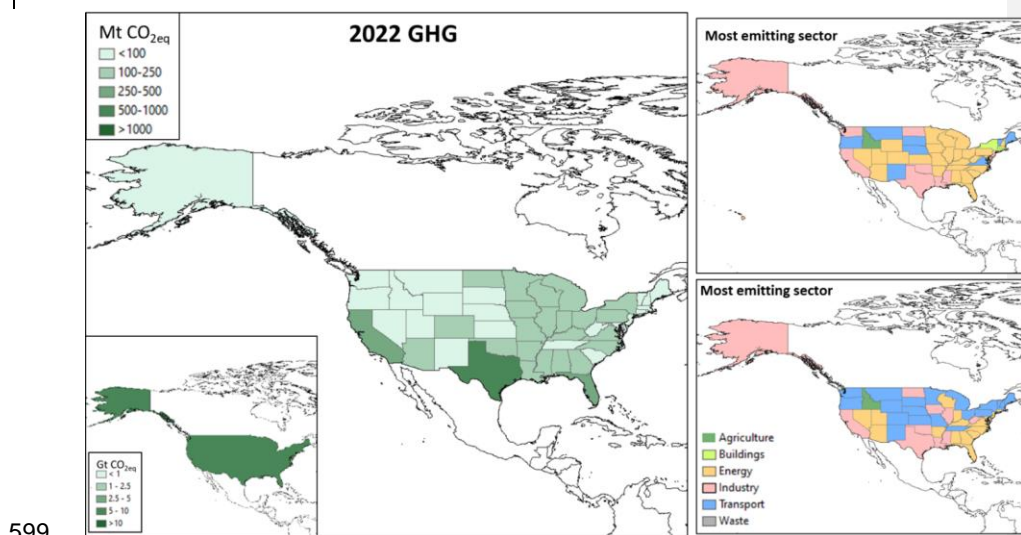
570 EDGAR_v8.0 [also](#) includes GHG emission estimates at the sub-national level [also](#) for the
 571 United States (i.e. estimates for each US state, [Figure-13](#)) [and](#), for each Chinese province and

each Indian state (Figure-14). Based on our analysis, Texas emitted 11.5 % of the total US GHG emissions in 2022, followed by California with a contribution of 7.7 % and Florida with a share of 4.6 %. In 1990, Texas and California were the most emitting states, followed by Ohio, Pennsylvania and Illinois. Over the past three decades, the sector with the highest share of GHG emissions at the state level over the United States has changed, with a shift from power generation and industry towards transport (see Figure-13).

In 2022, the five most emitting Chinese provinces contributed around 40 % of the China's total GHG emissions. These were Shandong (8.9 % of the country total), Guangdong (8.4 %), Jiangsu (7.4 %), Hebei (6.6 %) and Nei Mongol (6.5 %), findings consistent with other literature studies addressing provincial CO₂ and GHG emissions in China (Jiang et al., 2019; Zhang et al., 2020). In 1990, the top five emitting provinces were Shandong (8.1 %), Hebei (6.5 %), Jiangsu (6.2 %), Henan (5.9 %) and Nei Mongol (5.8 %), contributing around 30 % to the China's total GHG emissions.

In 2022, five Indian states emitted around 50 % of the country's total GHG emissions, namely Maharashtra (11.8 %), Tamil Nadu (11.7 %), Uttar Pradesh (8.1 %), Gujarat (8.0 %) and Chhattisgarh (6.6 %). In 1990, the most emitting Indian states were Tamil Nadu (18.4 %), Maharashtra (9.5 %), Uttar Pradesh (9.3 %), West Bengal (6.6 %) and Andhra Pradesh (6.0 %). Compared with the US and European cases, a different picture is found over the Asian domain in terms of the top emitting sectors at the sub-national level (Figure-14). The effect of the India's economic growth and its transition from an agricultural economy towards a more industrialised economy can be seen in Figure-14 (right panels). As a result, the sectors with the highest share of GHG emissions changed from agriculture (in 1990) to energy and industry (in 2022) over China and India, with the exception of some a few regions (e.g. Tamil Nadu, Assam, Jammu and Kashmir, Uttarakhand) which that still had an agriculture-based economy in 2022. This type of information and analysis is instrumental for the definition of effective sector-specific climate change mitigation actions at the sub-national level.

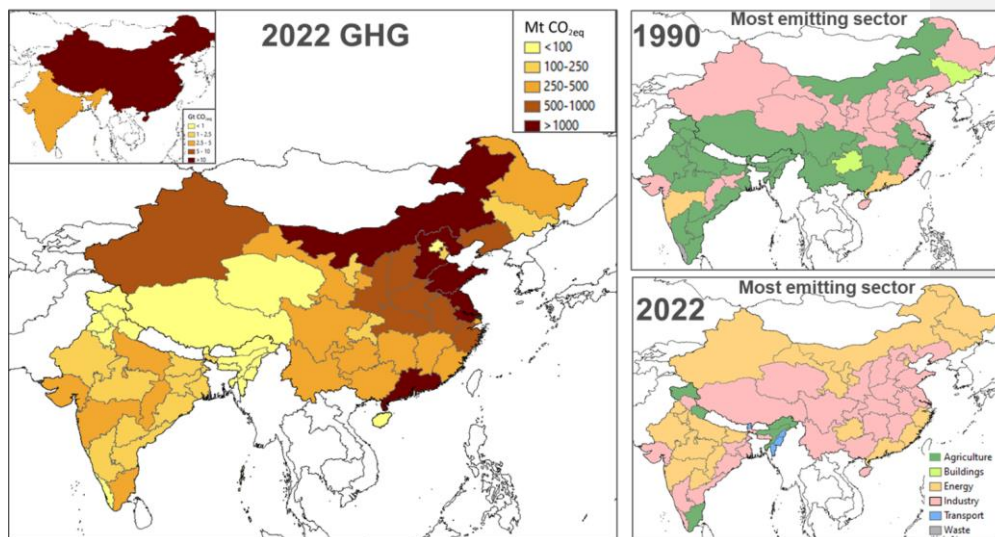
Formatted: Font: Subscript, Ligatures: None



599

600 Figure 13 – 2022 GHG emissions at the sub-national level in the United States are represented (left panel)
 601 and the sector with the highest contribution to total emissions in 1990 and 2022 for each US state (is shown
 602 in the maps on the right panels).

Formatted: Font: Ligatures: None



603 Figure 14 – 2022 GHG emissions at the sub-national level over the Asian domain, with a focus on China
 604 and India, (left panel) and the sector with the highest contribution in 1990 and 2022 for each Chinese
 605 province and Indian province/state (is shown in the maps on the right panels).
 606

607 7. Data availability

608 The EDGAR_v8.0 GHG global emission maps can be freely accessed at
 609 <https://doi.org/10.2905/b54d8149-2864-4fb9-96b9-5fd3a020c224> (Crippa, 2023a). The
 610 EDGAR_v8.0 subnational emissions can be accessed at [doi:10.2905/D67EEDA8-C03E-4421-95D0-0ADC460B9658](https://doi.org/10.2905/D67EEDA8-C03E-4421-95D0-0ADC460B9658)
 611 <https://doi.org/10.2905/D67EEDA8-C03E-4421-95D0-0ADC460B9658> (Crippa et al., 2023b). All data can also be accessed through the EDGAR
 612 website at https://edgar.jrc.ec.europa.eu/dataset_ghg80 and
 613 https://edgar.jrc.ec.europa.eu/dataset_ghg80_nuts2 (last access: November 2023).
 614

Field Code Changed

Field Code Changed

615 Data are made available as emission grid maps for each species and for total GHGs as .txt and
 616 .nc files with emissions expressed in tonnes substance per 0.1° x degree x 0.1° per degree/year.
 617 Emission fluxes are available as .nc files and they are expressed in kilograms substance per /m²
 618 per /second. Emission maps are available both as both total and sector-specific emissions.

Formatted: Font: Ligatures: None

Formatted: Font: Superscript, Ligatures: None

619 8. Conclusions

620 Climate targets are often set at the global and national levels; however, their implementation
 621 may occur at the subnational level. It is therefore of the utmost relevance to develop sub-
 622 national GHG emission estimates for policy development and to monitor the progress towards
 623 climate targets or to evaluate their impacts.

624 This work summarises the main updates developed with into the Emissions Database for Global
 625 Atmospheric Research (EDGAR) for what concerning the use of high-resolution and up-to-

626 date spatial information to improve the global geospatial disaggregation of GHG emissions at
627 ~~the~~ sub-national level. Having accurate and up-to-date sector-specific ~~GHG-emission~~ global
628 maps ~~of GHG emissions~~ at high spatial resolution ($0.1^\circ \times 0.1^\circ$ ~~degrees~~) is instrumental for the
629 design of effective climate ~~change~~ mitigation options beyond (inter)national climate targets.
630 EDGAR_v8.0 spatial proxies include globally consistent spatial data derived, for example, from
631 the Global Energy Monitor, the ~~Global Human Settlements Layer~~ ~~GHSL~~ work, satellite-based
632 information ~~to-for~~ ~~computing~~ ~~heating degree day~~ ~~HDDs~~ or ~~to-for~~ ~~identifying~~ hot-spots from
633 agricultural activities, ~~the~~ ~~STEAM~~ ~~model~~ for ship tracking and many other global datasets. The
634 use of satellite data to improve the EDGAR spatial proxies represents a successful cooperation
635 between bottom-up inventory compilers and the Earth observation community, and the
636 ~~possibility-potential~~ to integrate relevant satellite-based datasets and statistical information. In
637 addition, EDGAR_v8.0 integrates spatial information from local databases (e.g. EPRTR for
638 Europe, EIA data for the ~~United States~~) when including ~~data~~ more detailed ~~data~~ than that
639 available in global databases.

640 Continuous updates and improvements ~~of-in~~ the spatial data used to downscale national
641 emissions over the global grid are required to ~~best-accurately~~ represent ~~the evolution-of-trends~~
642 ~~in~~ emission sources and their location. The strength and uniqueness of the EDGAR work ~~are~~
643 ~~arises from~~ ~~associated-with~~ its global coverage and consistency in computing and representing
644 emissions for all countries, thus becoming a reference for many countries with limited
645 capabilities ~~for-to~~ ~~estimate their~~ ~~emissions-estimation~~. However, several challenges are
646 associated with the use of global databases ~~of information~~, in particular dealing with the
647 collection of point sources. Therefore, the use of local data, if available, is recommended when
648 performing analysis at the highest spatial resolution (e.g. at ~~the city~~ ~~scale-level-etc~~).

649 A further improvement ~~within~~ EDGAR is related ~~with-to~~ the inclusion of sub-national
650 information, representing a unique feature ~~to-that can~~ address in a consistent way the evaluation
651 of spatial patterns in ~~the evolution-of-trends in~~ sub-national GHG emissions. Such spatial
652 resolution and sub-national sector-specific variability ~~sets-prepares~~ the ground for the
653 production of city-level emission data records, as used, for example, in the Urban Centre
654 Database (https://ghsl.jrc.ec.europa.eu/ghs_stat_ucdb2015mt_r2019a.php). In this paper, a few
655 case studies are presented, with ~~the~~ main focus on the European case where the EDGAR sub-
656 national data are regularly used as input ~~for-to~~ the ~~European U~~ ~~s~~ Semesters and contribute to
657 climate action territorial and cohesion policies through the EU ~~c~~ Cohesion ~~r~~ Reports.

658 The EDGAR v8.0 data release ~~is-providing~~ an improved GHG dataset that ~~couldan~~ be useful
659 for air quality modellers, but also ~~for~~ policy-makers willing to analyse subnational GHG
660 emission patterns. Future EDGAR activities will focus on delivering an updated dataset for air
661 pollutants, including the latest spatial information made available through this work.

662

663 9. Acknowledgements

664 We are grateful to William Becker for the thorough review and proofreading of this manuscript.
665 The views expressed in this publication are those of the author(s) and do not necessarily reflect
666 the views or policies of the European Commission. All emissions, except ~~for~~ CO₂ emissions
667 from fuel combustion, are from the EDGAR (~~Emissions Database for Global Atmospheric~~
668 ~~Research~~) ~~c~~ Community GHG database comprising IEA-EDGAR CO₂, EDGAR CH₄, EDGAR

Formatted: Font: Ligatures: None

Formatted: Font: (Default) Times New Roman, Subscript, Ligatures: None

Formatted: Font: (Default) Times New Roman, Subscript, Ligatures: None

Formatted: Font: (Default) Times New Roman, Subscript, Ligatures: None

669 N₂O and EDGAR F-gases version 8.0 (2023). [The IASI-NH₃ catalogue](#) was updated in the
670 framework of the [European Space Agency](#) World Emission project ([https://www.world-](https://www.world-emission.com/)
671 [emission.com/](https://www.world-emission.com/)). The [Université libre de Bruxelles](#) also gratefully acknowledges support from
672 the TAPIR project (Air Liquide Foundation).

673 **References**

674 Ahsan, H., Wang, H., Wu, J., Wu, M., Smith, S. J., Bauer, S., Suchyta, H., Olivie, D., Myhre,
675 G., Matsui, H., Bian, H., Lamarque, J. F., Carslaw, K., Horowitz, L., Regayre, L., Chin, M.,
676 Schulz, M., Skeie, R. B., Takemura, T., and Naik, V.: The Emissions Model Intercomparison
677 Project (Emissions-MIP): quantifying model sensitivity to emission characteristics, *Atmos.*
678 *Chem. Phys.*, 23, 14779-14799, 10.5194/acp-23-14779-2023, 2023.

679 Alessandrini, A., Guizzardi, D., Janssens-Maenhout, G., Pisoni, E., Trombetti, M., and Vespe,
680 M.: Estimation of shipping emissions using vessel Long Range Identification and Tracking
681 data, *Journal of Maps*, 13, 946-954, 10.1080/17445647.2017.1411842, 2017.

682 Atalla, T., Gualdi, S., and Lanza, A.: A global degree days database for energy-related
683 applications, *Energy*, 143, 1048-1055, <https://doi.org/10.1016/j.energy.2017.10.134>, 2018.

684 Bieser, J., Aulinger, A., Matthias, V., Quante, M., and Denier van der Gon, H. A. C.: Vertical
685 emission profiles for Europe based on plume rise calculations, *Environmental Pollution*, 159,
686 2935-2946, <https://doi.org/10.1016/j.envpol.2011.04.030>, 2011.

687 CEIP: Inventory Review 2021 Review of emission data reported under the LRTAP
688 Convention,
689 https://www.ceip.at/fileadmin/inhalte/ceip/00_pdf_other/2021/inventoryreport_2021.pdf, Last
690 Access: August 2023., 2021.

691 Clarisse, L., Van Damme, M., Clerbaux, C., and Coheur, P. F.: Tracking down global NH₃
692 point sources with wind-adjusted superresolution, *Atmos. Meas. Tech.*, 12, 5457-5473,
693 10.5194/amt-12-5457-2019, 2019.

694 Crippa, M., Guizzardi, D., Pagani, F., and Pisoni, E.: GHG Emissions at sub-national level,
695 European Commission, Joint Research Centre (JRC) [Dataset] doi:10.2905/D67EEDA8-
696 C03E-4421-95D0-0ADC460B9658 PID: [http://data.europa.eu/89h/d67eeda8-c03e-4421-](http://data.europa.eu/89h/d67eeda8-c03e-4421-95d0-0adc460b9658)
697 [95d0-0adc460b9658](http://data.europa.eu/89h/d67eeda8-c03e-4421-95d0-0adc460b9658), 2023b.

698 Crippa, M., Guizzardi, D., Pisoni, E., Solazzo, E., Guion, A., Muntean, M., Florczyk, A.,
699 Schiavina, M., Melchiorri, M., and Hutfilter, A. F.: Global anthropogenic emissions in urban
700 areas: patterns, trends, and challenges, *Environmental Research Letters*, 16, 074033,
701 10.1088/1748-9326/ac00e2, 2021.

702 Crippa, M., Guizzardi, D., Muntean, M., Schaaf, E., Dentener, F., van Aardenne, J. A., Monni,
703 S., Doering, U., Olivier, J. G. J., Pagliari, V., and Janssens-Maenhout, G.: Gridded emissions
704 of air pollutants for the period 1970–2012 within EDGAR v4.3.2, *Earth Syst. Sci. Data*, 10,
705 1987-2013, 10.5194/essd-10-1987-2018, 2018.

706 Crippa, M., Guizzardi, D., Pagani, F., Banja, M., Muntean, M., Schaaf, E., Becker, W.,
707 Monforti-Ferrario, F., Quadrelli, R., Riquez Martin, A., Taghavi-Moharamli, P., Köykkä, J.,
708 Grassi, G., Rossi, S., Brandao De Melo, J., Oom, D., Branco, A., San-Miguel, J., and Vignati,

Formatted: Font: (Default) Times New Roman, Subscript, Ligatures: None

Formatted: Font: (Default) Times New Roman, Subscript, Ligatures: None

Formatted: Default Paragraph Font, Font: (Default) Times New Roman, Ligatures: None

Formatted: Default Paragraph Font, Font: (Default) Times New Roman, Ligatures: None

Formatted: Default Paragraph Font, Font: (Default) Times New Roman, Ligatures: None

Formatted: Default Paragraph Font, Font: (Default) Times New Roman, Ligatures: None

Formatted: Font: Ligatures: None

709 E.: GHG emissions of all world countries, Publications Office of the European Union,
710 Luxembourg, doi:10.2760/953322, JRC134504, 2023c.

711 Crippa, M., Guizzardi D., Pagani F., Banja M., Muntean M., Schaaf E., Becker, W., Monforti-
712 Ferrario F., Quadrelli, R., Risquez Martin, A., Taghavi-Moharamli, P., Grassi, G., Rossi, S.,
713 Brandao De Melo, J., Oom, D., Branco, A., San-Miguel, J., Vignati, E.: EDGAR v8.0
714 Greenhouse Gas Emissions, European Commission, Joint Research Centre (JRC) [Dataset] doi:
715 10.2905/b54d8149-2864-4fb9-96b9-5fd3a020c224 PID: [http://data.europa.eu/89h/b54d8149-
716 2864-4fb9-96b9-5fd3a020c224](http://data.europa.eu/89h/b54d8149-2864-4fb9-96b9-5fd3a020c224), 2023a.

717 de Meij, A., Krol, M., Dentener, F., Vignati, E., Cuvelier, C., and Thunis, P.: The sensitivity
718 of aerosol in Europe to two different emission inventories and temporal distribution of
719 emissions, Atmos. Chem. Phys., 6, 4287-4309, 10.5194/acp-6-4287-2006, 2006.

720 Elvidge, C. D., Baugh, K., Zhizhin, M., Hsu, F. C., and Ghosh, T.: Supporting international
721 efforts for detecting illegal fishing and GAS flaring using viirs, 2017 IEEE International
722 Geoscience and Remote Sensing Symposium (IGARSS), 23-28 July 2017, 2802-2805,
723 10.1109/IGARSS.2017.8127580,

724 EPRT: E-PRTR database v18, [https://www.eea.europa.eu/data-and-maps/data/member-
725 states-reporting-art-7-under-the-european-pollutant-release-and-transfer-register-e-prtr-
726 regulation-23/european-pollutant-release-and-transfer-register-e-prtr-data-
727 base/eptr_v9_csv.zip](https://www.eea.europa.eu/data-and-maps/data/member-states-reporting-art-7-under-the-european-pollutant-release-and-transfer-register-e-prtr-regulation-23/european-pollutant-release-and-transfer-register-e-prtr-data-base/eptr_v9_csv.zip), 2020.

728 European Commission: Cohesion in Europe towards 2050 - Eighth report on economic, social
729 and territorial cohesion, doi: 10.2776/624081, 2022.

730 European Commission: GHSL Data Package 2023, Publications Office of the European Union,
731 Luxembourg, JRC133256, doi:10.2760/098587, 2023.

732 European Union: European Commission, Joint Research Centre (JRC), EDGAR (Emissions
733 Database for Global Atmospheric Research) Community GHG database, comprising IEA-
734 EDGAR CO₂, EDGAR CH₄, EDGAR N₂O and EDGAR F-gases version 8.0 (2023). Unless
735 otherwise noted, all material owned by the European Union is licensed under the Creative
736 Commons Attribution 4.0 International (CC BY 4.0) licence. This means that reuse is allowed,
737 provided that appropriate credit is given and any changes are indicated, 2023.

738 EUROSTAT: [https://ec.europa.eu/eurostat/web/gisco/geodata/reference-data/administrative-
739 units-statistical-units/nuts](https://ec.europa.eu/eurostat/web/gisco/geodata/reference-data/administrative-units-statistical-units/nuts), 2021.

740 Feng, L., Smith, S. J., Braun, C., Crippa, M., Gidden, M. J., Hoesly, R., Klimont, Z., van Marle,
741 M., van den Berg, M., and van der Werf, G. R.: The generation of gridded emissions data for
742 CMIP6, Geosci. Model Dev., 13, 461-482, 10.5194/gmd-13-461-2020, 2020.

743 Freire, S., MacManus, K., Pesaresi, M., Doxsey-Whitfield, E., and and Mills, J.: Development
744 of new open and free multi-temporal global population grids at 250 m resolution, Geospatial
745 Data in a Changing World, Association of Geographic Information Laboratories in Europe
746 (AGILE), 2016.

747 Global Energy Monitor: Global Coal Mine Tracker,
748 <https://globalenergymonitor.org/projects/global-coal-mine-tracker/>, 2022a.

749 Global Energy Monitor: Global Coal Plant Tracker,
750 <https://globalenergymonitor.org/projects/global-coal-plant-tracker/>, 2022b.

751 Global Energy Monitor: Global Gas Plant Tracker,
752 <https://globalenergymonitor.org/projects/global-gas-plant-tracker/>, 2022c.

753 Global Energy Monitor: Global steel plant tracker,
754 <https://globalenergymonitor.org/projects/global-steel-plant-tracker/>, 2022d.

755 Guevara, M., Enciso, S., Tena, C., Jorba, O., Dellaert, S., Denier van der Gon, H., and Pérez
756 García-Pando, C.: A global catalogue of CO₂ emissions and co-emitted species from power
757 plants, including high-resolution vertical and temporal profiles, *Earth Syst. Sci. Data*, 16, 337-
758 373, 10.5194/essd-16-337-2024, 2024.

759 Hoesly, R. M., Smith, S. J., Feng, L., Klimont, Z., Janssens-Maenhout, G., Pitkanen, T.,
760 Seibert, J. J., Vu, L., Andres, R. J., Bolt, R. M., Bond, T. C., Dawidowski, L., Kholod, N.,
761 Kurokawa, J. I., Li, M., Liu, L., Lu, Z., Moura, M. C. P., O'Rourke, P. R., and Zhang, Q.:
762 Historical (1750–2014) anthropogenic emissions of reactive gases and aerosols from the
763 Community Emissions Data System (CEDS), *Geosci. Model Dev.*, 11, 369-408, 10.5194/gmd-
764 11-369-2018, 2018.

765 IEA-EDGAR CO₂: A component of the EDGAR (Emissions Database for Global Atmospheric
766 Research) Community GHG database version 8.0 (2023) including or based on data from IEA
767 (2022) Greenhouse Gas Emissions from Energy, www.iea.org/data-and-statistics, as modified
768 by the Joint Research Centre, 2023.

769 Jalkanen, J. P., Johansson, L., Kukkonen, J., Brink, A., Kalli, J., and Stipa, T.: Extension of an
770 assessment model of ship traffic exhaust emissions for particulate matter and carbon monoxide,
771 *Atmos. Chem. Phys.*, 12, 2641-2659, 10.5194/acp-12-2641-2012, 2012.

772 Janssens-Maenhout, G., Crippa, M., Guizzardi, D., Muntean, M., Schaaf, E., Dentener, F.,
773 Bergamaschi, P., Pagliari, V., Olivier, J. G. J., Peters, J. A. H. W., van Aardenne, J. A., Monni,
774 S., Doering, U., Petrescu, A. M. R., Solazzo, E., and Oreggioni, G. D.: EDGAR v4.3.2 Global
775 Atlas of the three major greenhouse gas emissions for the period 1970–2012, *Earth Syst. Sci.*
776 *Data*, 11, 959-1002, 10.5194/essd-11-959-2019, 2019.

777 Jiang, J., Ye, B., and Liu, J.: Peak of CO₂ emissions in various sectors and provinces of China:
778 Recent progress and avenues for further research, *Renewable and Sustainable Energy Reviews*,
779 112, 813-833, <https://doi.org/10.1016/j.rser.2019.06.024>, 2019.

780 Johansson, L., Jalkanen, J.-P., and Kukkonen, J.: Global assessment of shipping emissions in
781 2015 on a high spatial and temporal resolution, *Atmospheric Environment*, 167, 403-415,
782 <https://doi.org/10.1016/j.atmosenv.2017.08.042>, 2017.

783 Kuenen, J., Dellaert, S., Visschedijk, A., Jalkanen, J. P., Super, I., and Denier van der Gon, H.:
784 CAMS-REG-v4: a state-of-the-art high-resolution European emission inventory for air quality
785 modelling, *Earth Syst. Sci. Data*, 14, 491-515, 10.5194/essd-14-491-2022, 2022.

786 Kuramochi, T., Roelfsema, M., Hsu, A., Lui, S., Weinfurter, A., Chan, S., Hale, T., Clapper,
787 A., Chang, A., and Höhne, N.: Beyond national climate action: the impact of region, city, and
788 business commitments on global greenhouse gas emissions, *Climate Policy*, 20, 275-291,
789 10.1080/14693062.2020.1740150, 2020.

790 Melchiorri, M.: The global human settlement layer sets a new standard for global urban data
791 reporting with the urban centre database, 10, 10.3389/fenvs.2022.1003862, 2022.

792 NOAA: Visible Infrared Imaging Radiometer Suite (VIIRS),
793 <https://www.ngdc.noaa.gov/eog/viirs.html>, Latest Access: July 2023, 2017.

794 Pesaresi, M. and Politis, P.: GHS-BUILT-S R2023A - GHS built-up surface grid, derived from
795 Sentinel2 composite and Landsat, multitemporal (1975-2030), European Commission, Joint
796 Research Centre (JRC), <http://data.europa.eu/89h/9f06f36f-4b11-47ec-abb0-4f8b7b1d72ea>,
797 doi:10.2905/9F06F36F-4B11-47EC-ABB0-4F8B7B1D72EA, 2023.

798 Schiavina, M., Melchiorri, M., and Pesaresi, M.: GHS-SMOD R2023A - GHS settlement
799 layers, application of the Degree of Urbanisation methodology (stage I) to GHS-POP R2023A
800 and GHS-BUILT-S R2023A, multitemporal (1975-2030), European Commission, Joint
801 Research Centre (JRC), PID: [http://data.europa.eu/89h/a0df7a6f-49de-46ea-9bde-
802 563437a6e2ba](http://data.europa.eu/89h/a0df7a6f-49de-46ea-9bde-563437a6e2ba), doi:10.2905/A0DF7A6F-49DE-46EA-9BDE-563437A6E2BA, 2023a.

803 Schiavina, M., Freire, S., Carioli, A., and MacManus, K.: GHS-POP R2023A - GHS population
804 grid multitemporal (1975-2030). European Commission, Joint Research Centre (JRC),
805 <http://data.europa.eu/89h/2ff68a52-5b5b-4a22-8f40-c41da8332cfe>, doi:10.2905/2FF68A52-
806 5B5B-4A22-8F40-C41DA8332CFE, 2023b.

807 Spinoni, J., Vogt, J. V., Barbosa, P., Dosio, A., McCormick, N., Bigano, A., and Füssel, H. M.
808 J. I. J. o. C.: Changes of heating and cooling degree-days in Europe from 1981 to 2100, 38,
809 e191-e208, <https://doi.org/10.1002/joc.5362>, 2018.

810 Thunis, P., Kuenen, J., Pisoni, E., Bessagnet, B., Banja, M., Gawuc, L., Szymankiewicz, K.,
811 Guizardi, D., Crippa, M., Lopez-Aparicio, S., Guevara, M., De Meij, A., Schindlbacher, S.,
812 and Clappier, A.: Emission ensemble approach to improve the development of multi-scale
813 emission inventories, EGUsphere, 2023, 1-27, 10.5194/egusphere-2023-1257, 2023.

814 US EIA: US Coal mines, <https://atlas.eia.gov/datasets/eia::coal-mines-1/explore>, 2022a.

815 US EIA: US Energy Atlas, [https://atlas.eia.gov/datasets/eia::power-
816 plants/explore?location=41.629235%2C-118.496000%2C3.79](https://atlas.eia.gov/datasets/eia::power-plants/explore?location=41.629235%2C-118.496000%2C3.79), 2022b.

817 USGS: USGS Mineral Resources On-Line Spatial Data, <http://mrdata.usgs.gov/>, Last Access:
818 January 2019, 2019.

819 Van Damme, M., Clarisse, L., Whitburn, S., Hadji-Lazaro, J., Hurtmans, D., Clerbaux, C., and
820 Coheur, P.-F.: Industrial and agricultural ammonia point sources exposed, Nature, 564, 99-103,
821 10.1038/s41586-018-0747-1, 2018.

822 Wang, C., Corbett, J., and Firestone, J.: Improving Spatial Representation of Global Ship
823 Emissions Inventories, Environmental science & technology, 42, 193-199,
824 10.1021/es0700799, 2008.

825 World Bank: Global Gas Flaring Tracker Report, Last
826 <https://www.worldbank.org/en/programs/gasflaringreduction/global-flaring-data>,
827 Access: August 2023, 2023.

828 World Resources Institute: Global Power Plant Database, Global Energy Observatory, Google,
829 KTH Royal Institute of Technology in Stockholm, Enipedia, 2018.

830 WRI: Global Power Plant Database v1.3.0,
831 <https://datasets.wri.org/dataset/globalpowerplantdatabase>, 2021.

832 Zhang, X., Geng, Y., Shao, S., Dong, H., Wu, R., Yao, T., and Song, J.: How to achieve China's
833 CO2 emission reduction targets by provincial efforts? – An analysis based on generalized
834 Divisia index and dynamic scenario simulation, Renewable and Sustainable Energy Reviews,
835 127, 109892, <https://doi.org/10.1016/j.rser.2020.109892>, 2020.

836

837 Table 1 – Overview of updated spatial proxies in EDGAR_v8.0, including data sources
838 and methods.

Sector and spatial coverage	Old EDGAR proxies	New EDGAR proxies	Details of new EDGAR proxies	Time Period coverage	Data access
Power plants (global)	CARMA_v3.0 (not any more longer available): 2004, 2009, 2014, fuel type derived from plant capacity (assumption)	Global Coal Plant Tracker / Global Oil and Gas Plant Tracker (Global Energy Monitor)	Coal, Gas	1970–2050	https://globalenergymonitor.org/projects/global-coal-plant-tracker/ and https://globalenergymonitor.org/projects/global-gas-plant-tracker/ (2022)
		Global Power Plant Database v1.3.0	Biomass, Other, Oil		https://datasets.wri.org/dataset/globalpowerplantdatabase
		US EIA	USA power plants, all fuels	All	https://atlas.eia.gov/datasets/eia::power-plants/explore?location=41.629235%2C-118.496000%2C3.79
		CARMA_v3.0	Autoproducers, missing countries	2004, 2009, 2014	http://carma.g/
All other industries (Europe)	EPRTTR v4*	European Pollutant Release and Transfer Register (EPRTTR), v18	All industries and waste plants (with the exception of power plants, iron and steel plants, and coal mines)	2007–2017	https://www.eea.europa.eu/data-and-maps/data/member-states-reporting-art-7-under-the-european-pollutant-release-and-transfer-register-eprtr-regulation-23/european-pollutant-release-and-transfer-register-eprtr-data-base/eprtr_v9_csv.zip
Iron and steel (global)	In-house EDGAR	Global steel plant tracker (Global Energy Monitor)		1970–2050	https://globalenergymonitor.org/projects/global-steel-plant-tracker/

Coal mines (global)	USGS—derived proxies, Global Energy Observatory (China)	Global Coal Mine Tracker (Global Energy Monitor)	Brown and hard coal, surface and underground	1970–2050	https://globalenergymonitor.org/projects/global-coal-mine-tracker/
		Global Energy Monitor + EIA (Energy Information Administration)	United States: all fuels, more precise opening and closing years	1970–2050	https://atlas.eia.gov/datasets/eia:coal-mines-1/explore
		EDGAR old proxy	For missing countries	Key years	
Flaring (global)	NOAA-NDGC (2015) VIIRS data (https://www.ngdc.noaa.gov/eog/viirs.html)	Global Gas Flaring Tracker Report (2023)	Used for both venting and flaring activities	2012–2022	https://www.worldbank.org/programs/flaringreduction/global-flaring-data
Small-scale combustion (global)	Global Human Settlements Layer (GHSL) (1975, 1990, 2000, 2015)	Global Human Settlements Layer (GHSL) data package 2023 + Heating Degree-Days (HDDs) from ERA5	For all fuels	Population every 5 years from 1975 to 2030; HDDs every year from 1970 to 2022	https://ghsl.jrc.ec.europa.eu/ghs_pop2023.php and https://cds.climate.copernicus.eu/cdsapp#!/dataset/reanalysis-era5-single-levels?tab=form
Small-scale combustion in agriculture (global)-Rural population	Global Human Settlements Layer (GHSL) (1975, 1990, 2000, 2015)	Global Human Settlements Layer (GHSL) data package 2023, including GHSMOD R2023A – GHSL settlement layers + Heating Degree-Days (HDDs) from ERA5	For small-scale combustion in agriculture, which are mostly associated with rural areas.	Population every 5 years from 1975 to 2030; HDDs every year from 1970 to 2022	https://ghsl.jrc.ec.europa.eu/ghs_pop2023.php , and https://cds.climate.copernicus.eu/cdsapp#!/dataset/reanalysis-era5-single-levels?tab=form
Intensive livestock and fertiliser-manufacturing industries (global)	-Livestock density maps	European Space Agency World Emission project; intensive livestock point sources were taken from EPRTR_v18 for Europe.	For intensive livestock and fertiliser industry, gap filling with livestock density map	-2008–2022	https://www.world-emission.com/
Gap-filling of industrial activities (global)	Population based	Built-up for non-residential areas from Global	It is used entirely when no information is available or for attributing a fraction of	Every 5 years from	https://ghsl.jrc.ec.europa.eu/g

Formatted: Font: Italic, Ligatures: None

839
840

		Human Settlements GHSL data package 2023	emissions which that i was not allocated to point sources-	1975 to 2030	hs_buS2023.php
International shipping	In-house EDGAR proxy based on LRIT—long-range identification and tracking and Wang et al. (2007) and Alessandrini, Trombe et al. (2017)	STEAM (Ship Traffic—Emission Assessment Model)	Based on CO ₂ emissions for multiple -vessels and multiple -years-	2000–2018	Jalkanen et al. (2012); Johansson al. (2017)

Formatted: Subscript, Ligatures: None

Formatted: Not Highlight

Formatted: Ligatures: None